Žune Ba-F epithermal deposit : mineralogical and geochemical characteristics

Roglić, Martin

Master's thesis / Diplomski rad

2022

Degree Grantor / Ustanova koja je dodijelila akademski / stručni stupanj: **University of Zagreb, Faculty of Mining, Geology and Petroleum Engineering / Sveučilište u Zagrebu, Rudarsko-geološko-naftni fakultet**

Permanent link / Trajna poveznica: https://urn.nsk.hr/urn:nbn:hr:169:184241

UNIVERSITY OF ZAGREB
FACULTY OF MINING, GEOLOGY AND PETROLEUM ENGINEERING
Graduate study of Geology

ŽUNE Ba-F EPITHERMAL DEPOSIT: MINERALOGICAL AND GEOCHEMICAL CHARACTERISTICS

Master's thesis

Martin Roglić
G404

Zagreb, 2022.

KLASA: 602-04/21-01/275
URBROJ: 251-70-15-21-2
U Zagrebu, 5. 1. 2022.

Martin Roglić, student

RJEŠENJE O ODOBRENJU TEME

Na temelju vašeg zahtjeva primljenog pod KLASOM 602-04/21-01/275, URBROJ: 251-70-15-21-1 od 3. 12. 2021. priopćujemo vam temu diplomskog rada koja glasi:

ŽUNE Ba-F EPITHERMAL DEPOSIT: MINERALOGICAL AND GEOCHEMICAL CHARACTERISTICS

Za mentoricu ovog diplomskog rada imenuje se u smislu Pravilnika o izradi i obrani diplomskog rada Prof. dr. sc. Sibila Borojević Šoštarić nastavnik Rudarsko-geološko-naftnog-fakulteta Sveučilišta u Zagrebu.

Mentorica:

(potpis)

Prof. dr. sc. Sibila Borojević Šoštarić

(titula, ime i prezime)

Predsjednik povjerenstva za završne i diplomske ispite:

(potpis)

Doc. dr. sc. Zoran Kovač

(titula, ime i prezime)

Prodekan za nastavu i studente:

(potpis)

Izv. prof. dr. sc. Borivoje Pašić

(titula, ime i prezime)

ACKNOWLEDGMENTS

My gratitude goes to my mentor, prof. Sibila Borojević Šoštarić, PhD, who provided me the opportunity to do this master's thesis under her wing. For her enthusiasm and love for geology that kept my morale up during time of writing this thesis. I also thank her for all the time set aside, giving me useful advices and whose critical eye to detail kept this research on the right path.

To assistant, mag. geol. Tomislav Brenko, I thank for helping me with microscopic analysis as well as interpreting data obtained with geochemical one. To Michaela Hrušková Hasan, PhD and Vinko Baranašić I thank for helping me prepare the samples for XRD analysis. Same as to technician Mario Valent for preparing the thin sections.

My field research would not be possible without assoc. prof. Jasna Orešković, PhD and Saša Kolar, who showed me how certain geophysical exploration methods work and applying theory to practice. For making geological maps and profiles, as in-charge for structural geology, I thank to assoc. prof. Aleksej Milošević, PhD from Faculty of Mining, Banja Luka.

Last but not least, my special thanks go to my family and friends who supported me during this academic journey and provided me strength to see this through.

University of Zagreb
Faculty of Mining, Geology and
Petroleum Engineering

Master's thesis

ŽUNE Ba-F EPITHERMAL DEPOSIT: MINERALOGICAL AND GEOCHEMICAL CHARACTERISTICS

MARTIN ROGLIĆ

Thesis completed in: University of Zagreb
Faculty of Mining, Geology and Petroleum engineering
Institute of Mineralogy, Petrology and Mineral Resources
Pierottijeva 6, 10000 Zagreb

Abstract

The Žune Ba-F epithermal deposit is located in Ljubija ore field (NW Bosnia and Herzegovina) within the Upper Paleozoic dolostone. Dolostone is fresh to partly limonitized and has massive, homogenous structure. Geochemical composition exhibits high CaO (30.24–32.38 mass. %), MgO (16.47–17.35 mass. %) and LOI (44.60–45.58 mass. %) while having low SiO_2 (1.33–3.65 mass. %), Al_2O_3 (0.27–0.74 mass. %) and BaO (0.02–0.83 mass. %) contents. Contact zone between dolostone and ore mineralization is characterized with primary accessory minerals tremolite magnesiochloritoid, topaz (pyknite), epidote, pyrite and rutile which point to forming temperatures generally above 300°C and pressure up to 2 kbars. The ore body of Žune deposit is predominantly vein-type of mineralization, whereas breccia-type is less common with barite and fluorite as main ore minerals. These two main ore minerals are deposited first in veinlets, alongside quartz but relationship with sulphides could indicate their near-simultaneous crystallization. Mineralized samples are characterized by high CaO (6.30–66.03 mass. %) and BaO (3.92–50.23 mass. %) contents, and increased concentrations of SO_3 (2.05–26.22 mass. %) and fluor (2.01–22.88 mass. %). The rare earth element (REE) spectra (5.73 to 166.01 ppm) are dominated by enrichment of light lanthanides. Elevated Sr (> 1 mass. %), Sm (up to 118 ppm) and Eu (up to 44 ppm) contents follow trend of higher amount of barite in samples while fluorite-rich samples are characterized by enrichment of Y (up to 41 ppm) and HREE, and depletion of LREE. XRD analysis conducted on four ore samples confirmed presence of dolomite, barite and fluorite, respectively. From primary accessory minerals chloritoid was detected. Based on variable REE concentrations, negative Ce and Yb anomaly, Žune deposit geochemically belongs to category of fluorite deposits associated with carbonate sedimentary rocks.

Keywords: barite-fluorite deposit, Dinarides, mineralogy, geochemistry, REE, ore-forming conditions

Thesis contains: 47 pages, 5 tables, 16 figures and 54 references.

Original in: English

Thesis deposited in: Library of Faculty of Mining, Geology and Petroleum Engineering, Pierottijeva 6, Zagreb

Supervisor: Prof. Sibila Borojević Šoštarić, PhD

Reviewers: Prof. Sibila Borojević Šoštarić, PhD
Assoc. prof. Jasna Orešković, PhD
Assoc. prof. Aleksej Milošević, PhD

Date of defense: January 14th, 2022.

Sveučilište u Zagrebu
Rudarsko-geološko-naftni fakultet

Diplomski rad

ŽUNE Ba-F EPITERMALNO LEŽIŠTE: MINERALOŠKE I GEOKEMIJSKE KARAKTERISTIKE

MARTIN ROGLIĆ

Diplomski rad izrađen: Sveučilište u Zagrebu
Rudarsko-geološko-naftni fakultet
Zavod za mineralogiju, petrologiju i mineralne sirovine
Pierottijeva 6, 10000 Zagreb

Sažetak

Žune Ba-F epitermalno ležište dio je Ljubijskog rudnosnog bazena (SZ Bosna i Hercegovina), smješteno u gornjo paleozojskim dolomitima kao stijenama domaćinima. Dolomit je uglavnom svjež do mjestimično limonitiziran, te ima masivnu, homogenu teksturu. Geokemijska analiza otkriva prisutnost viših koncentracija CaO (30.24–32.38 mass. %), MgO (16.47–17.35 mas. %) i LOI (44.6–45.58 mas. %), ali isto tako i niske koncentracije SiO_2 (1.33–3.65 mas. %), Al_2O_3 (0.27–0.74 mas. %) i BaO (0.02–0.83 mas. %). Kontaktna zona između dolomita i mineralizacije u ležištu karakterizirana je primarnim akcesornim mineralima tremolitom, magneziokloritoidom, topazom (piknitom), epidotom, piritom i rutilom koji upućuju na temperature iznad 300°C i tlakove oko 2 kbar-a, kao uvjete formiranja. Rudno tijelo, s baritom i fluoritom kao glavnim rudnim mineralima, dominantno je žilnog, te u manjoj mjeri brečastog tipa. Barit i fluorit kristalizirali su prvi, uz kvarc u žilama, ali odnos sa sulfidima mogao bi upućivati na njihovu gotovo istovremenu kristalizaciju. Uzorci u kojima se javlja mineralizacija karakterizirani su visokim koncentracijama CaO (6.30–66.03 mas. %) i BaO (3.92–50.23 mas. %) te relativno nižim koncentracijama SO_3 (2.05–26.22 mas. %) i fluora (2.01–22.88 mass. %). Od elemenata rijetkih zemalja (ERZ) dominiraju lake rijetke zemlje. Povišena koncentracija Sr (> 1 mas. %), Sm (do 118 ppm) i Eu (do 44 ppm) prati povećan sadržaj barita u uzorcima, dok su fluoritom bogati uzroci karakterizirani povišenim koncentracijama Y (do 41 ppm), elemenata teških rijetkih zemalja, te osiromašeni na elementima lakih rijetkih zemalja. XRD analiza provedena na četiri uzorka potvrdila je prisutnost dolomita, barita i fluorita, dok je od primarnih akcesornih minerala kloritoid detektiran. Na temelju varijabilnog sadržaja ERZ-a i negativne Ce i Yb anomalije, Žune kao ležište geokemijski pripada svjetskim ležištima fluorita vezanim za karbonatne sedimentne stijene.

Ključne riječi: baritno-fluoritno ležište, Dinaridi, mineralogija, geokemija, rudnonosni uvjeti formiranja

Diplomski rad sadrži: 47 stranica, 5 tablica, 16 slika i 54 reference.

Jezik izvornika: Engleski

Završni rad pohranjen: Knjižnica Rudarsko-geološko-naftnog fakulteta, Pierottijeva 6, Zagreb

Voditelj: Dr. sc. Sibila Borojević Šoštarić, redovita profesorica RGNF

Ocjenjivači: Dr. sc. Sibila Borojević Šoštarić, redovita profesorica RGNF
Dr. sc. Jasna Orešković, izvanredna profesorica RGNF
Dr. sc. Aleksej Milošević, izvanredni profesor RF, UNIBL

Datum obrane: 14. siječanj 2022.

TABLE OF CONTENTS

LIST OF TABLES

LIST OF FIGURES

1. Introduction

The Žune ore deposit is situated in the north-western part of Bosnia and Herzegovina, within the Central Dinarides. It is part of Ljubija ore field that includes four open pit mines (Adamuša, Tomašica, Omarska and Vidernjak) in an area of approximately 120 km^2 (**Palinkaš et al., 2016**). Except for iron, other commodities like zinc, lead, barite and fluorite were exploited in this area. Žune is a Ba-F epithermal type of deposit, implying near-surface forming conditions with shallow depths, lower temperatures and pressures alongside hydrothermal fluids circulating through the host rock. The biggest barite ore deposits in the Dinarides are located in the Mid-Bosnian Schist Mountains (MBSM) (**Jurković et al., 2010**). MBSM is one of four Paleozoic complexes (**Fig. 1-1**) whereas South-eastern Bosnia (SEB), Eastern Bosnia (EB) and Sana-Una are remaining three, where barite occurs. Žune barite-fluorite deposit is located within the Sana-Una river Paleozoic terrain, and represent a rare case of barite-fluorite mineralization within Dinarides. Barite and fluorite are the main ore minerals forming the ore body in this deposit. Barite ($BaSO_4$) is industrial mineral with high specific gravity which is predominantly used in petroleum industry as a weighting material during drilling, in medical industry and has wide variety of other applications. Fluorite (CaF_2), also known as fluorspar, is an important industrial mineral used in the metallurgical, ceramic and chemical industries. Fluorite occurs in different geological environments and deposit types, and commonly occurs as secondary mineral associated with the Early Paleozoic continental rift related deposits. Many geothermal fields and subterrestrial hydrothermal siderite-barite-polysulfide deposits were formed as a consequence of incipient magmatism and a high heat flow during early-intracontinental rifting of Pangea. **Magotra et al.** (**2017**) stated that fluorite associated with sedimentary rocks and Mississipi-valley type (MVT) deposit is characterized with low formation temperatures usually ranging between 100˚C and 150˚C, and variable salinities between 12 wt% eq NaCl to 22 wt% eq NaCl implying epigenetic formation conditions. In the Žune deposit, **Palinkaš et al.** (**2016**) pointed to ore forming fluids of $NaCl\text{-}CaCl_2\text{-}H_2O$ composition with highly variable salinity and homogenization temperature between 100 and 310°C referring to epithermal conditions.

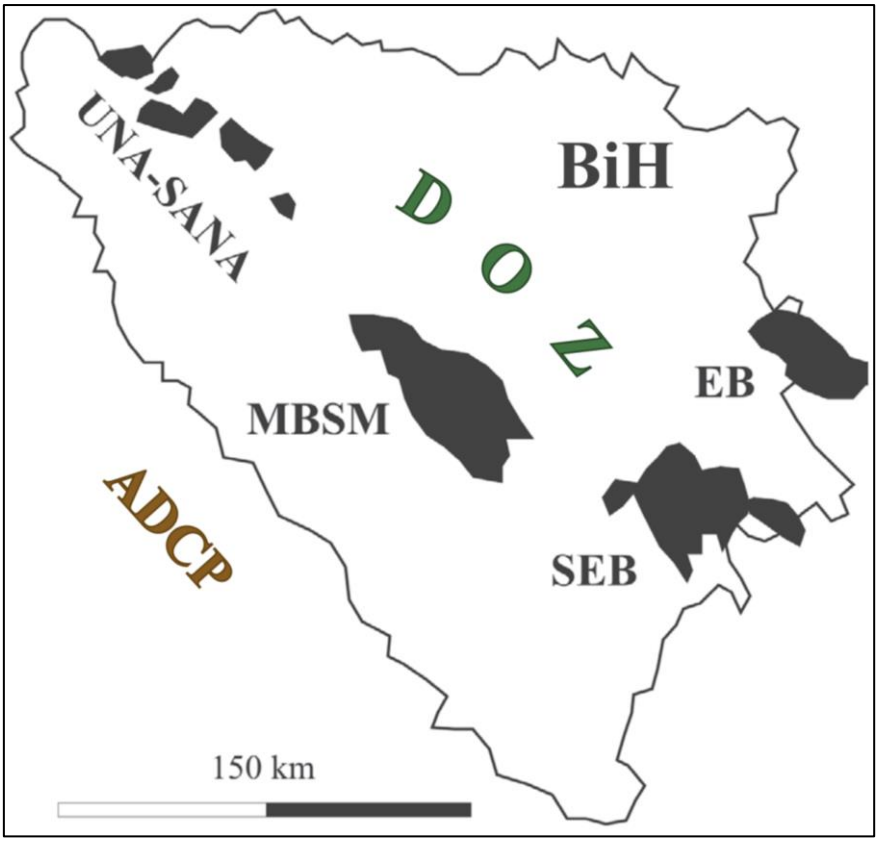

Figure 1-1. Position of the Paleozoic complex of Sana-Una, Mid-Bosnian Schist Mountains (MBSM), South-eastern Bosnia (SEB) and Eastern Bosnia (EB) with Dinaride ophiolite zone (DOZ) and Adriatic carbonate platform (ADCP) in Bosnia and Herzegovina (modified after **Jurković et al., 2010**).

The aim of this master's thesis is to conduct detailed mineralogical-petrographic, X-ray diffraction (XRD) and geochemical analysis on representative samples of the Upper Paleozoic rocks from the Žune ore deposit in which barite and fluorite occur. Petrographic analysis is conducted on 14 representative samples in order to determine relationship between mineral phases, as between dolostone and mineralization, where primary accessory minerals occur in the so called "contact zone" indicating specific ore-forming conditions. Petrographic analysis is also the basis on which 4 ore samples were selected for further XRD analysis to confirm the presence of certain mineral phases recognized in the thin sections. Ore-forming conditions and genesis of this barite-fluorite deposit have also been researched by the means of geochemical analysis, trace and rare earth elements and their enrichment in the host rock, barite and fluorite. These analyses are carried out and data are collected in order to comprehensively understand

the composition of ore-forming fluids and to determine the ore-forming epoch of this deposit in north-western Bosnia and Herzegovina. Besides analyses carried out, one of the main goals was to form a local geological map of the Žune deposit while conducting detailed geological field mapping and finally, to contribute to a better understanding of how this rare type deposit formed in framework of the Dinarides orogeny.

The research of the Žune Ba-F deposit for this master's thesis was conducted as a part of EIT RawMaterials project no. 17501-Invest RM. Invest RM: Multifactor model for investments in the raw material sector.

2. Geographical setting

The Žune deposit is located near small town of Žune, in the north-western part of Srpska region in Bosnia and Herzegovina (44.55˚N, 16.35˚E; **Fig. 2-1B**) at an altitude of 250 to 300 m above sea level. It belongs to municipality of Prijedor. Larger, more populated towns near Žune are Ljubija and Prijedor. Ljubija town is 2.5 km away from the Žune deposit, and Prijedor is about 14 km away. Kozara mountain is positioned NE from Žune, with highest peak Lisina at 978 m.a.s.l., and Majdanske mountain on SW with highest peak Glavica at 650 m.a.s.l.

Hydrographic network is relatively dense with biggest rivers Sana and Una that surround Žune deposit, Sana River from NNE and Una River from NW. The Sana River bifurcates into few smaller distributary channels that pass closer to the Žune deposit. Volar River, at north, bifurcates from Sana River to Bijelo Vrelo, Stankovac and Nedžak channel and Ljubija River that bifurcates from Sana River east from Volar channel, and later to Žunski stream passing near the deposit of Žune.

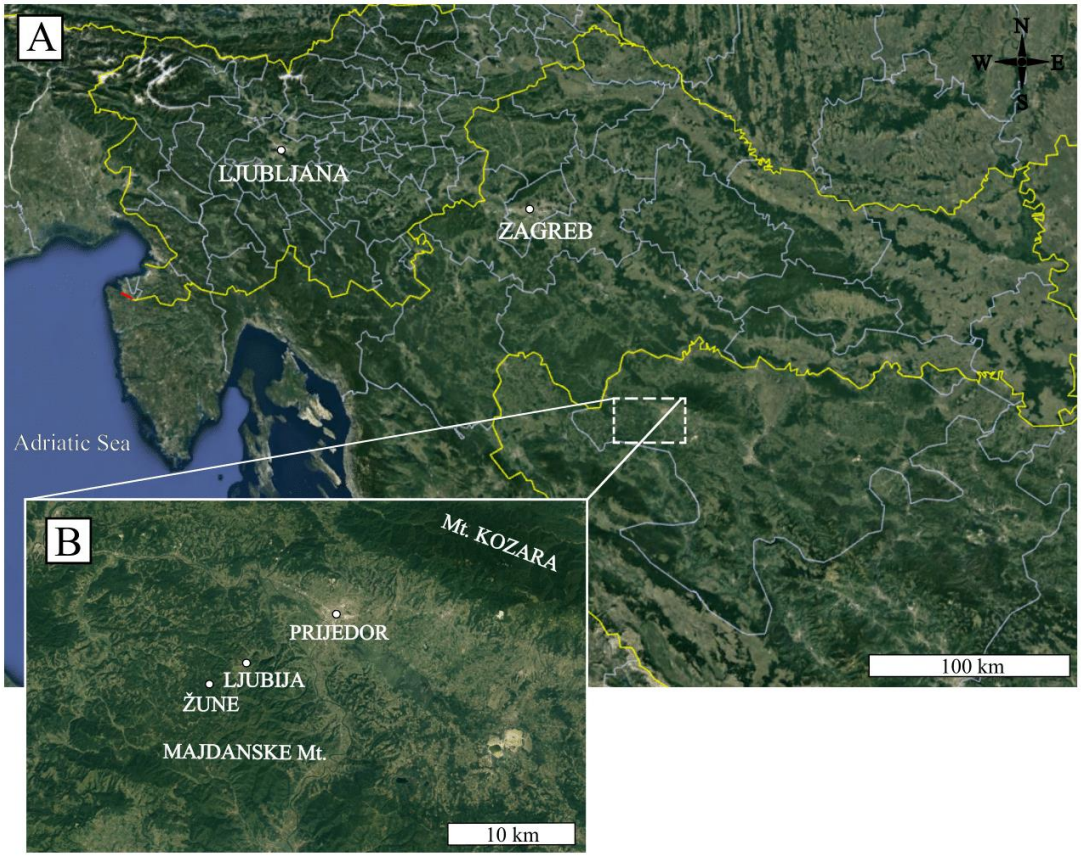

Figure 2-1. A) Geographical position of the study area in relation to other countries. Dashed line designates approximate location of study area; **B)** Detailed geographical position of the Žune deposit (https://earth.google.com/web/).

3. Geological setting

3.1. Regional geological setting

As a part of the Dinaric Variscan basement, Paleozoic complexes occur in the Internal Dinarides where they are included in the nappe structures by south-westward directed thrusting and are resting on the Adriatic carbonate platform units. Dinaric ophiolite zone is trusted onto Paleozoic complexes and represent their north-eastern border (**Pamić and Jurković, 2002**; **Fig. 3-1**). The same complexes in the Internal Dinarides also represent the south-eastern continuation of the Paleozoic complexes of the Eastern Alps.

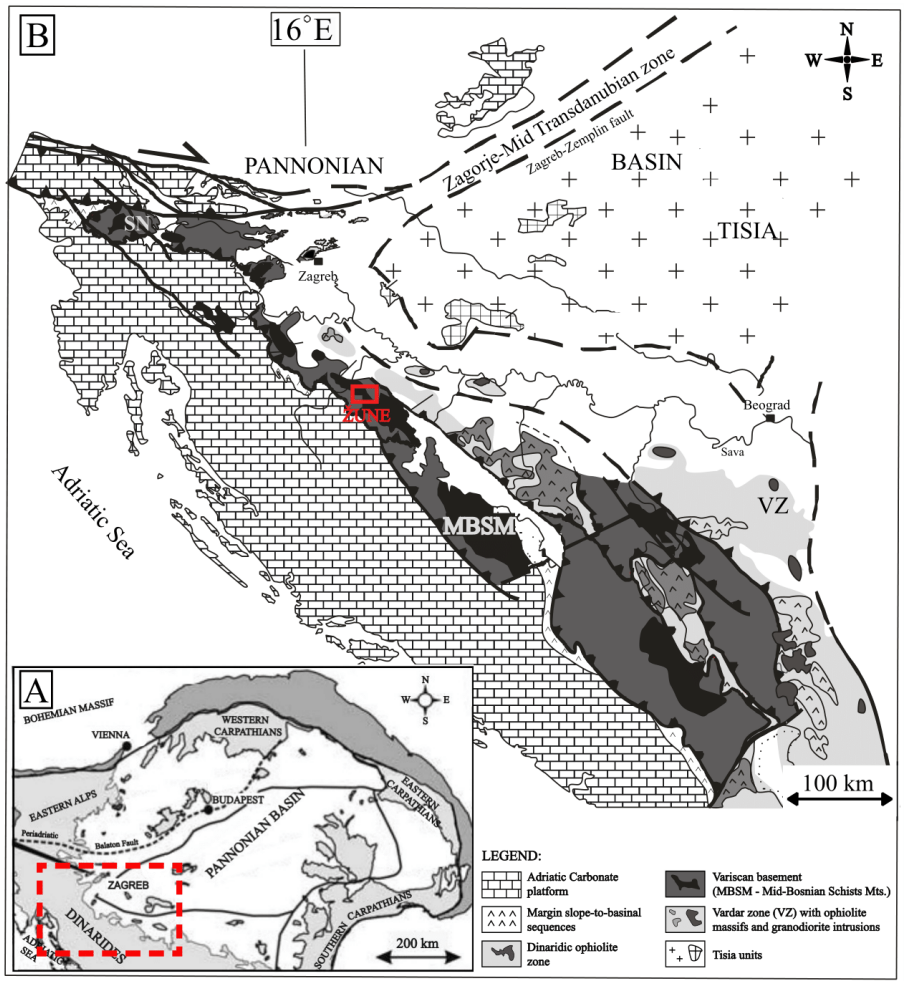

Figure 3-1. A) Simplified geological descriptive map of the Pannonian basin system indicating Dinarides position; **B)** Simplified geological map of major tectonostratigraphic units and zones in Dinarides with marked position of the Žune deposit (modified after **Pamić, 1993**; **Pamić et al., 1998**; **Schmid et al., 1998**; **Willingshofer, 2000**; **Tomljenović, 2002**).

One of those Paleozoic complexes where Žune deposit occur is Sana-Una Paleozoic (**Fig. 1-1**). It also belongs to the north-western part of the Dinaric Variscan basement units which are paleogeographically related to Apulia and Africa. This complex is located east of the Una River and is extended over the area from Novi Grad through Prijedor to Sanski Most, Budimlić Japra, Ključ and Mrkonjić Grad where the most widespread strata belong to the Javorik flysch formation (**Fig. 3-2**). The Una River also separates Sana Paleozoic from Banija, Croatia to the north-west. The boundaries of the Sana-Una Paleozoic are defined on the basis of anomalous contact with younger strata (north-eastern and south-western boundary), and in parts where tectonic elements are not expressed, the boundaries are defined on the basis of topographic

criteria (**Jurić, 1971**). The area features an interesting geological phenomenon due to the known and potential deposits of iron, occurrences of barite and other mineral raw materials.

The Sana-Una Paleozoic consists mostly out of Carboniferous flysch sequences (sensu **Karamata et al., 1997**), where **Majer** (**1964**) determined low and very low–grade metamorphic conditions (quartz–feldspars–sericite–chlorite–mica–ankerite assemblage). Ljubija deposits are set in its Carboniferous part belonging to the Javorik flysch formation, which is well exposed in the Adamuša and Tomašica opencast mines, where the majority of the mineral resources are emplaced within the olistostrome member (**Fig. 3-1**). The olistostrome unit contains metasomatic mineralization represented by siderite, ankerite, and fellow carbonates, and represent host-rocks for the largest iron deposits in Dinarides, the Ljubija deposit. Ljubija is huge siderite-barite-Pb-Zn sulphide ore deposit situated within the Sana-Una Paleozoic terrain. According to **Grubić et al.** (**2015**) the Javorik flysch formation is composed out of three members, the Pre-flysch and Lower flysch, Olistostrome member and Upper flysch.

Pre-Flysch and Lower Flysch member, as the basal units of the formation, consists of dark argillaceous schists in alternation with medium-grain sandstone. This member was probably formed in a deeper marine environment (**Grubić et al., 2015**).

Olistostrome member, with variable thickness between 100 to 300 m, formed of flysch matrix follows with embedded carbonate olistolithe segments, blocks and their mineralized parts. This member has a complex composition dominated by four groups of rocks: flysch matrix, carbonate olistolytic blocks, autoclastic melange, and partially or completely mineralized bodies. The olistostrome member was formed under deep-sea conditions that is found the core of the Sana antiform.

Pelitoid rocks of the Javorik flysch formation in the ore region have been altered, so what's left of them (recognized as e.g. sericite-chlorite-quartz argiloshist, carbonaceous sericite-quartz argiloshist etc.) belongs to the metamorphic group or to shales of the low degree of metamorphism. This points us that the rocks of the Javorik formation were, during the tectonic processing, brought into the conditions of epizonal regional metamorphism.

Within the Permian-Triassic clastites formation, with maximum thickness going up to 150 m, five members can be distinguished: i) Bobovica breccias, ii) white sandstones, iii) white and red

sandstones, iv) polygenous conglomerates and v) red sandstones and siltstones. The colourful Werfen strata are transgressively overlain by the limestones and dolomites, followed by the Ladinian volcanogenic-sedimentary porphyrite-chert formation. Of the younger sediments, only lacustrine Neogene-Quaternary formations can be found.

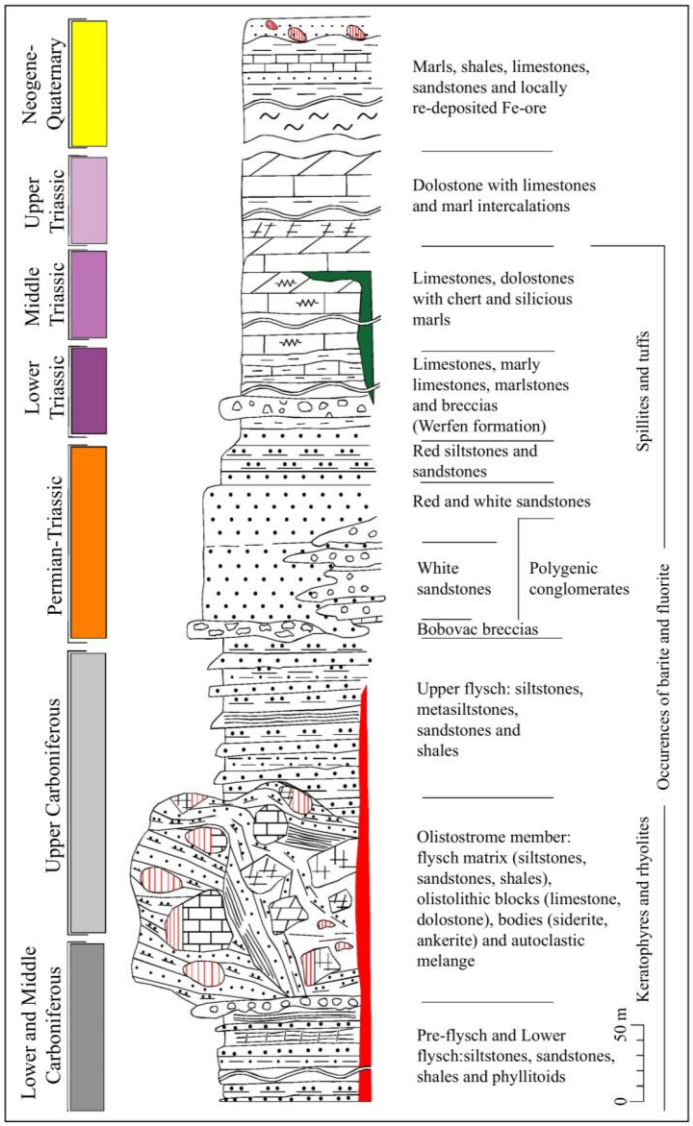

Figure 4-2. Schematic lithostratigraphic column of Sana-Una Paleozoic (modified after **Grubić et al., 2015**).

3.2. Local geological setting

Ba-F vein-type deposit Žune is situated in Upper Paleozoic dolostone and their close contact to Lower Triassic schists and sandstones (**Fig. 3-3**). Upper Paleozoic dolostone represent the host rock for this deposit. Barite-fluorite ore body is imprinted into porous dolostone along fault zone with general strike ESE-WNW.

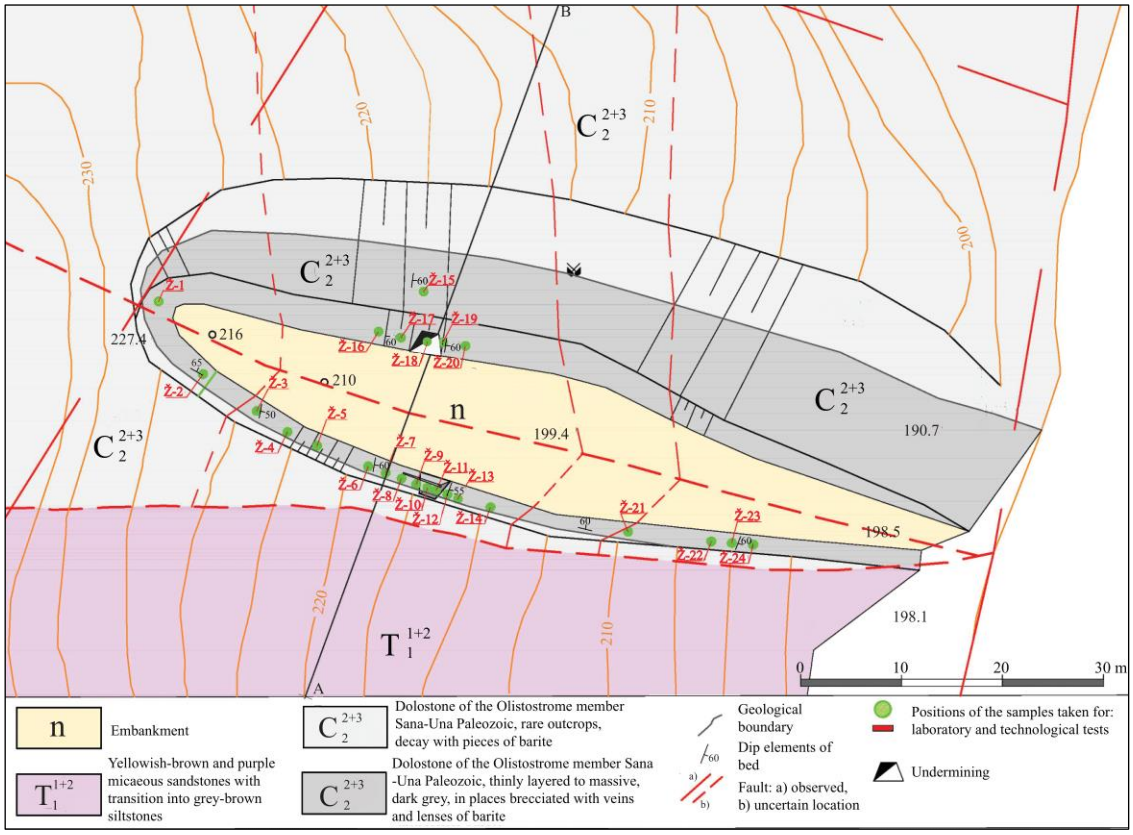

Figure 5-3. Geologic map of the Žune deposit with locations of collected samples and profile A – B transverse to deposit (**InvestRM dataset**).

It is positioned subvertical (**Fig. 3-4**) with thickness usually ranging from 3 to 10 m, but in the higher levels of the deposit it can go up to 20 m. Strike of the ore body can be followed up to 50 m in length. Sharp contact is common between the host rock and mineralized joints, although alterations and metasomatic repression have been noticed. The contact zone consists of metasomatically recrystallized host dolomite with strings of tiny barite veins and impregnations. The central part of vein consists of barite and fluorite. Barite is white in colour and occurs as massive in SW part of the deposit while in the NE part it is mostly porous. As such, it is exposed

in the middle part of the deposit. Within dolostone, barite is present in the shape of lenses and irregular bodies. Fluorite is violet to colourless with octahedral habit. It occurs as lenses within barite and dolostone but also as impregnation within dolostone itself. Accessory minerals include calcite, quartz, sulphides and sulfosalts (tetrahedrite, cinnabarite, pyrite, realgar) and Au (**Jeremić, 1958**). Upper part of the ore body is enriched with limonite of descendant origin. Deposit is covered on SW and NE part by soil cover that contains dolostone and barite boulders.

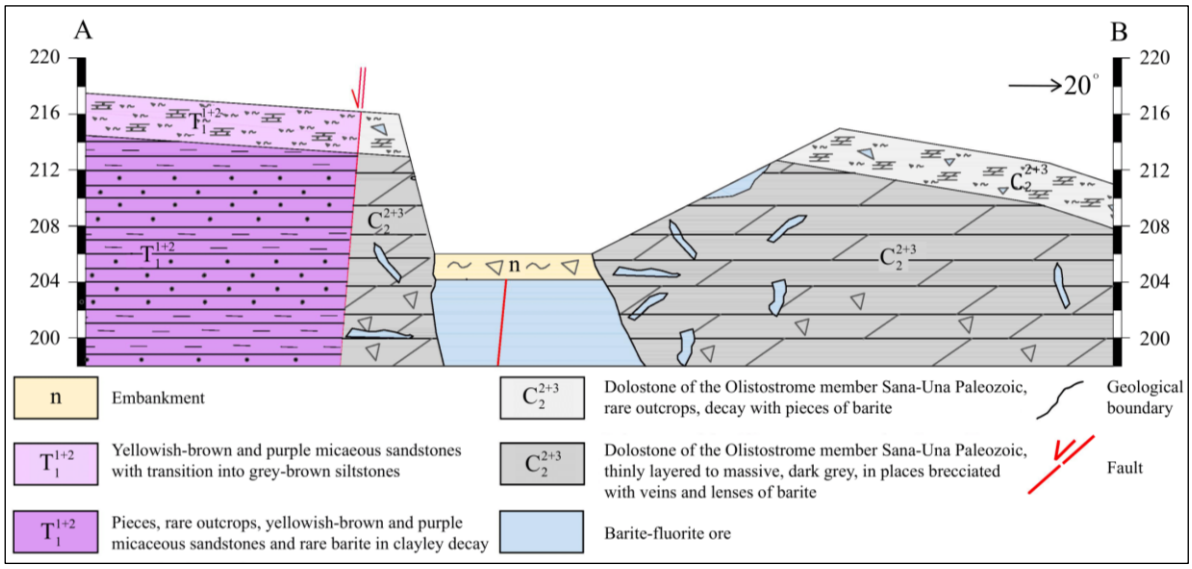

Figure 6-4. The cross section of the Žune deposit. Position of the barite-fluorite ore body (marked with light blue colour) within the Upper Paleozoic dolostone (C_2^{2+3}; grey in colour) (**InvestRM dataset**).

Together with other siderite-barite deposits in the Sana-Una Paleozoic terrains, Žune ore deposit was formed in Permo-Triassic period of time during and early stage of intracontinental rifting of Tethys. The source of heat and hydrothermal fluids were deeply placed thermal diapirs (**Palinkaš et al., 2016**).

4. Summary of research history of the Žune deposit as a part of Ljubija ore field

The first research on the Ljubija basin mineralization came from **Katzer** (**1910**) where he determined the relationship between Carboniferous limestone and siderite mineralization as a reaction contact.

Cissarz (**1951**) compare Ljubija ore deposits to hydrothermal deposits of Paleozoic age, related to deep magmatism.

Nöth (**1952**) suggests that irregular, vein-type Ljubija siderite ore bodies are intrusive-hydrothermal origin of younger Paleozoic age. Nöth concluded that Upper Paleozoic tectonic movements followed the formation of the Ljubija deposit.

Jeremić (**1958)** considers formation of the barite deposits of Sana-Una Paleozoic (Ljubija basin) via hydrothermal processes in Upper Paleozoic, as a consequence of batholith embedding.

Janković (**1974**, **1977**, **1982**, **1987**) and **Kubat** (**1982**) while studying Triassic deposits in central Bosnia and NW Montenegro, came to conclusion that mineralization in Foča, MBSM and Sana-Una Paleozoic is connected with Alpine-Triassic metallogeny followed by magmatism. **Janković** (**1987**) considers deposits in Dinarides (excluding the iron deposits in Macedonia) to be connected with intracontinental rifting and accompanied magmatic activity.

Palinkaš et al. (**1985**, **1988**, **1990**, **2010**, **2016**) analysed siderite-barite-sulphides deposits hosted by Upper Paleozoic complexes of the Inner Dinarides with emphasis put on Ljubija ore deposits. Genesis of the deposits was proposed to be hydrothermal-metasomatic or volcano-sedimentary with age of mineralization considered to be Variscan or younger Triassic. Žune ore deposit, together with other siderite-barite deposits in the Sana-Una Paleozoic terrains was considered to be formed in "Permo-Triassic" time during an early stage of intracontinental rifting of Tethys. Dry land facies, evaporate ponds and a disturbed thermal regime during initial phase of rifting, due to rifting magmatism, made favourable ore forming conditions for hydrothermal deposits (SEDEX) with well-developed feeder zone in the subterrestrial level. **Palinkaš** (**1990**) suggested origin of Žune ore body from a two phase region of the hydrothermal convective cell, and Ljubija from its lower margin. The depth of formation was determined between 200 and 500 m, depending on encountering lithostatic or hydrostatic pressure, based on PTX parameters of boiling fluids. Thus, boiling of ore forming fluids was recognized in Žune barite-fluorite ore body. Based on fluid inclusion studies, Laser Raman spectroscopy and bulk crush-leak analysis conducted in extensive study on Ljubija ore field, **Palinkaš et al.** (**2016**) presented renewed data on ore genesis, time of mineralization, temperature and chemistry of ore forming fluids.

5. Analytical methods and sampling

A total of twenty-four (Ž-1 to Ž-24) samples were collected from different locations in the Žune deposit (see **Figure 3-3**) out of which nineteen of them were examined microscopically. For the purposes of this master's thesis fourteen representative samples, chosen out of nineteen of them, were selected for the further analyses (n= 14; **Table 5-1**). The grain size was determined using a standard calibration micrometre scale.

Table 5-1. List of chosen representative samples and conducted analyses

Sample	Sample description	ICP-AAS	ICP-MS	XRD	Micropetrography
Ž-1	Dolostone	+	+		+
Ž-2		+	+		+
Ž-4		+	+		+
Ž-10		+	+		+
Ž-17		+	+		+
Ž-3	Ba-F vein type mineralization	+	+		+
Ž-11		+	+		+
Ž-16		+	+	+	+
Ž-19		+	+		+
Ž-20		+	+	+	+
Ž-5	Hydrothermal breccia			+	+
Ž-6					+
Ž-7		+	+	+	+
Ž-22					+

Detailed petrographic and geochemical (ICP-AAS and ICP-MS) analyses were made, alongside X-ray diffraction analysis (XRD) and description of hand specimens, as seen in **Table 5-1**.

Polarized light microscopy is a fundamental method for determining rocks' mineral paragenesis and relationship between certain mineral phases within, in order to classify the same rock but also to get an insight in rock-forming conditions and its alterations processes. Thin sections of nineteen samples were examined microscopically, with special emphasis put on representative fourteen of them. All samples were cut in thin plates with diamond saw after which their size was adjusted to the dimensions of cover glass. Canadian balsam (refractive index n= 1.537) was used for making microscope slides. Final thickness of the samples is very thin, about 30 μm, so polarized light can pass through the minerals in the thin section and their interference colours

would be the same within the different thin sections. Microscopic photographs were taken using the LEICA MICROSYSTEMS 020-522 101 DM/LSP polarization microscope in the Institute of Mineralogy, Petrology and Mineral Resources at the Faculty of Mining, Geology and Petroleum Engineering, University of Zagreb. The grain size was determined using a standard calibration micrometre scale.

X-ray diffraction (XRD) is an instrumental technique used to identify any crystalline substances, most such as minerals. X-rays are electromagnetic waves with wavelength of 10^{-10} m or 1Å. When an X-ray beam hits the sample and is diffracted, we can measure the distances between the planes of the atoms that constitute the sample by applying Bragg's Law:

$$n\lambda = 2d\sin\theta$$

Where the integer n is the order of the diffracted beam, λ is the wavelength of the incident X-ray beam, d (d-spacings) is the distance between adjacent of atoms and is θ the angle of incidence of the X-ray beam. The characteristic set of d-spacings generated in typical X-ray scan can provide a unique "fingerprint" of the mineral phase or phases in the sample. The mineralogical composition of four samples (n= 4; **Table 5-1**) was determined by XRD. Micropetrographical and geochemical analysis were conducted prior to XRD, based on which samples were selected for this analysis. Samples were homogenized in an agate grinding set to produce the powder fraction. A Malvern PanAnalytical vertical X–ray goniometer (type X'Pert MPD) was used, equipped with Cu tube and graphite crystal monochromator with the following experimental conditions: 45 kV, 40 mA, primary beam divergence automatic, irradiated length 0.5 mm, continuous scan (step 0.0131303º 2Q/s). Obtained spectra were analysed using X'Pert HighScore plus 2.1 PANalytical B.V. software.

Geochemical whole rock major and trace element analyses of Žune deposit rocks (n= 11; **Table 5-1**) were performed at the MSALabs Laboratory, Langley, Canada. Whole rock major elements were analysed by inductively coupled plasma–atomic emission spectrometry (ICP–AES), while trace elements including rare earth elements were determined by inductively coupled plasma–mass spectrometry (ICP–MS). Lithium metaborate/tetraborate fusion and dilute nitric digestion was used for decomposition of samples (0.2 g). Loss on ignition (LOI) was determined by weight difference after ignition at 1000°C. In addition, a separate 0.5 g split was digested in Aqua Regia and analysed by ICP-MS to determine the contents of precious and base metals.

Fluor and sulphide trioxide (SO_3) (**F*** and **SO_3***; **Table 6-1**) contents of were stehiometrically calculated based on the contents of other major oxides. Fluor content was determined based on the calcium and magnesium contents. Both CaO and MgO were expressed as moles by dividing their geochemical contents with their molecular mass and then subtracted. Excess of CaO moles was again converted to mass. % and expressed as Ca. Fluor content was calculated by dividing excess Ca with 2.055, which represents Ca to F ratio in fluorite (**Slovenec, 2002**). Contents of SO_3 were based on estimation of **Slovenec** (**2002**) that barite minerals consist of 65.70 mass. % BaO and 34.30 mass. % SO_3. From there the BaO/SO_3 conversion factor equals 1.915. Therefore, SO_3 contents were derived by dividing BaO contents with conversion factor.

Microelements and REEs were analysed using the GCD Toolkit in R language (**Janoušek et al., 2006**). Their contents were normalized to chondrite (**Anders and Grevesse, 1989**) and to Upper Continental Crust (**Taylor and McLennan, 1995**) and further plotted on the suitable diagrams. For more precise and distinguishing geochemical correlation of data, hierarchical clustering method was implemented using joint tree diagrams. Data was presented in the form of joint tree diagrams where the correlation of 29 variables is plotted. Hierarchical plotting of data was conducted using Statistica 12 (**StatSoft Inc., 2012**). As the main distance measure between the geochemical variables, the Euclidean distance was chosen for this study. Sample groups are connected with a linkage rule. The linkage process and grouping are repeated until all variables are connected wherefore the variables showing greatest similarity are grouped first.

6. Results

6.1. Petrographic analysis

Twenty-four samples collected from the Žune deposit can be divided into three groups, depending on how mineralization occurs: i) the host rock-dolostone; ii) hydrothermal breccia and iii) Ba-F vein type mineralization. Contact zone between dolostone and ore mineralization is characterized with primary accessory minerals present.

6.1.1. The host rock-dolostone

Dolostone, macroscopically has massive, homogeneous structure. It is mostly dark grey in colour (**Fig. 6-1A**) but in the minority of the samples colour can vary to light grey (**Fig. 6-1B**). Dolostone primary possess massive structure, though it occurs in three samples (Ž-5, Ž-6, Ž-7 and Ž-22) as part of breccia alongside barite and fluorite. It may also contain fluorite impregnation. Despite being fresh in most of the samples, the dolostone is also partly weathered, with limonitization occurring. This alteration completely affects samples Ž-9 and Ž-14, present in form of orange to brownish layers. Veinlets present within dolostone are more common in the proximity of the ore mineralization, occupying up to 15 vol. % of dolostone. Thickness of veinlets ranges from 1.00 to 5.75 mm.

Micropetrographical study of the host rock reveals the presence of relatively weathered, anhedral to subhedral mineral grains of dolomite (**Fig. 6-2A**, **6-2B**). Dolomite mineral grains make up most of dolostone with negligible amount of muscovite. **Dolomite** mineral grains show distinct relief changes and have poor to no visible cleavage. Extinction is parallel to cleavage (if present). Dimensions of dolomite grains range from 0.008 to 1.20 mm. Due to being partly weathered and crushed with cavities filled with fluorite, quartz or secondary carbonates, it has lower porosity values. The contact between dolomite and the veinlets filled with fluorite, barite and quartz, is long and regular.

Muscovite mineral grains have anhedral to subhedral grain form as they exhibit distinctive change in relief and cleavage is present. The extinction is parallel to the cleavage. Dimensions of the muscovite mineral grains vary from 0.004 to 0.18 mm. Interference colours go up to order II blue to pink.

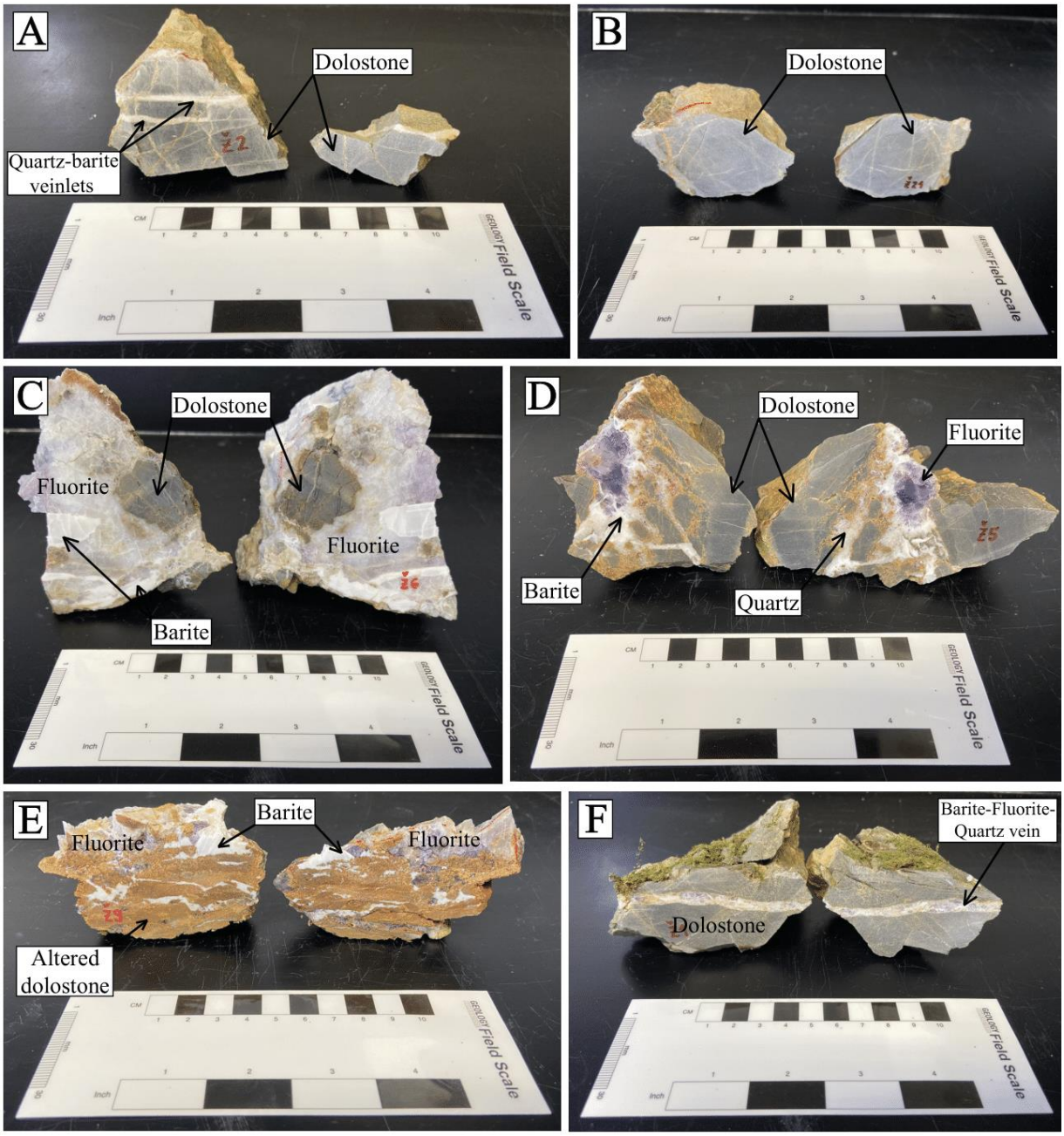

Figure 7-1. Hand specimens of Ž-2, Ž-21, Ž-6, Ž-5, Ž-9 and Ž-1 sample. **A)** Dolostone, dark grey in colour is intersected with quartz-barite veinlets in Ž-2 sample; **B)** Dolostone, light grey in colour intersected with very thin veinlets in Ž-21 sample**; C)** Ž-6 sample representing first of three hydrothermal breccia samples consisting out of fluorite in highest amount and followed by barite and dolostone; **D)** Ž-5 sample, dolostone-barite-fluorite-quartz hydrothermal breccia; **E)** Completely altered dolostone in Ž-9 sample with barite-fluorite veinlets intersecting; **F)** Barite-fluorite-quartz thin vein cutting grey coloured dolostone in Ž-1 sample.

6.1.2. Contact zone mineralogy

Contact zone between dolostone and ore mineralization is characterized with primary accessory minerals that occur on contact, within or near borders of the veinlets and dolostone. These primary accessory minerals are tremolite, magnesiochloritoid, topaz (pyknite), epidote, pyrite and rutile.

Tremolite commonly occurs as fibrous aggregates on contact between quartz with fluorite and secondary carbonates but is also found included in quartz grains (**Fig. 6-2C**). Being colourless to having a pale green elementary colour, tremolite often exhibits pleochroism from pale green to green and pale brown colour. High interference colours of II order blue to red are observed under analyser (+ N). Tremolite occupies up to 1 vol. % of thin sections.

Magnesiochloritoid (Mg-chloritoid) is always found as radially-shaped aggregates on contact between quartz and fluorite with dolomite or is incorporated within quartz grains (**Fig. 6-2C**). It shows pleochroism in light green colour and has white interference colour of I order with grains exhibiting high relief. Mg-chloritoid occupies up to 2 vol. % of thin sections.

Pyknite is a variety of fine grained **topaz**, but also occurs in dense aggregates of prismatic to acanthine crystals. In this case pyknite is present in shape of acicular mineral grains. It has brown elementary colour with pleochroism going from light to dark brown. Pyknite mineral grains have medium to high relief and are often found included in quartz mineral grains (**Fig. 6-2F**). Dimensions of pyknite mineral grains range from 0.003 to 0.17 mm. It occupies up to 1 vol. % of thin sections.

Epidote is common on dolostone-veinlets border present as granular aggregates or individual mineral grains which have a characteristically high relief. It has pale green elementary colour and high interference colour yellow to red of II order (**Fig. 6-2D**). Dimensions of epidote mineral grains vary from 0.02 to 0.16 mm. Epidote occupies up to 1 vol. % of thin sections.

Pyrite, opaque in thin section, has subhedral to euhedral, cubic and pyritohedral grain form (**Fig. 6-2F**) and is often found on dolostone-veinlets contact. Dimension of pyrite mineral grains range from 0.002 to 0.25 mm. Pyrite, besides present on dolostone-veinlets contact, is found on

the edges of other mineral grains or as small accumulations within them. It often alters to limonite. Pyrite occupies up to 1 vol. % of thin sections.

Rutile, alongside pyrite, represents the heavy mineral assemblage of the deposit. Rutile mineral grains are characterized with dark brown to green elementary colour and high relief. Dimensions of rutile mineral grains vary from 0.02 to 0.18 mm. It is present in negligible amount occupying less than 1 vol. % of thin sections.

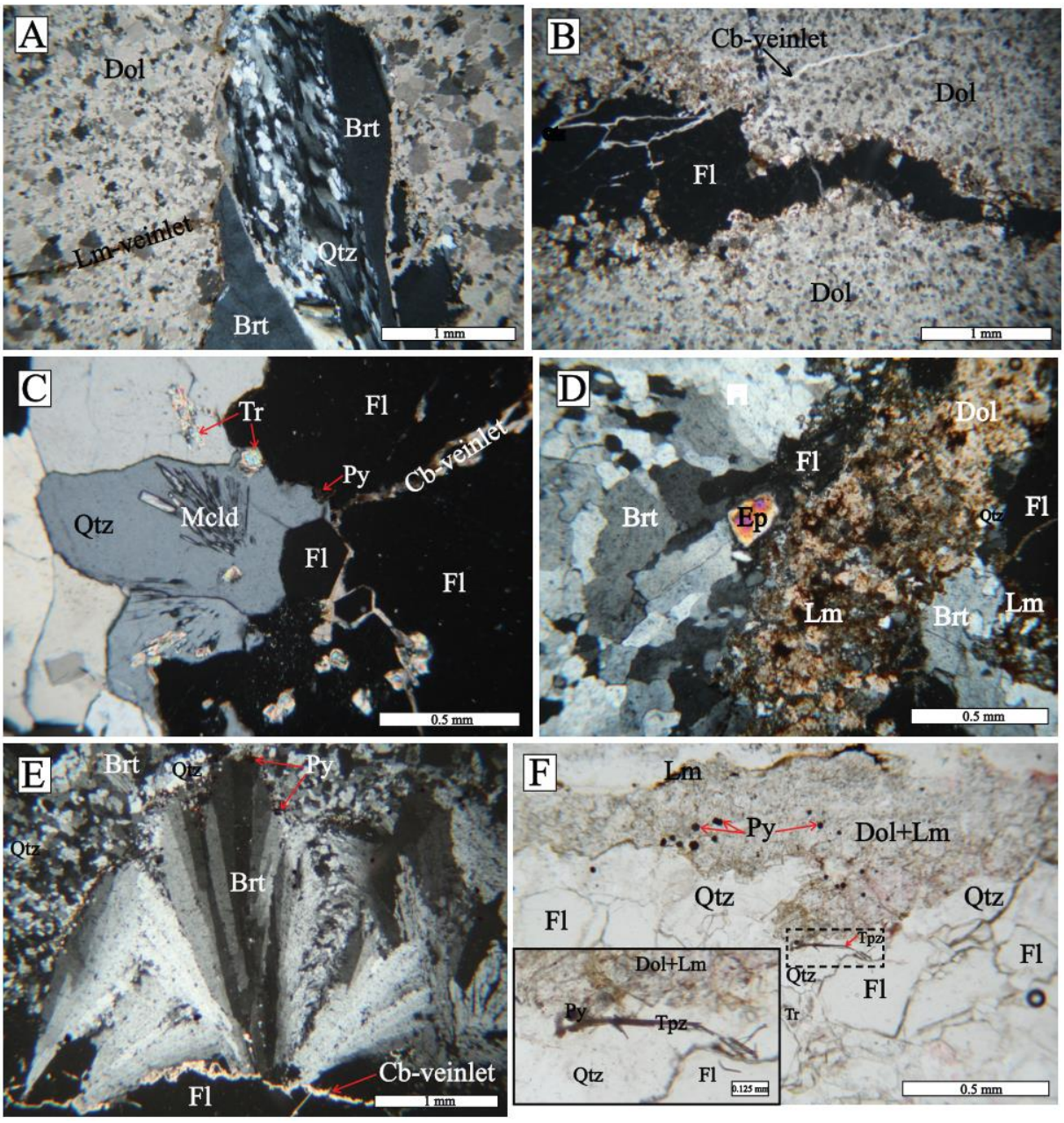

Figure 8-2. A) Microscopic photograph of Ž-2 sample (+ N). Quartz-barite veinlet hosted by dolostone consisted out of relatively weathered dolomite grains; **B)** Microscopic photograph of Ž-22 sample (+ N). Fluorite veinlet hosted by dolostone consisted out of relatively weathered dolomite grains; **C)** Microscopic photograph of Ž-5 sample (+ N). Radially-shaped aggregate of Mg-chloritoid incorporated in quartz, alongside fibrous aggregates of tremolite also included in quartz and on quartz-fluorite contact; **D)** Microscopic photograph of Ž-9 sample (+ N). Epidote, exhibiting high interference colours, on fluorite-barite-dolomite contact; **E)** Microscopic photograph of Ž-3 sample (+ N). Fan-shaped aggregates of barite surrounded with fine-grained barite and quartz; **F)** Microscopic photograph of Ž-17 sample. Acicular mineral grains of pyknite (topaz) incorporated in quartz mineral grain. Euhedral pyrite present with limonitized dolomite. Abbreviations: Brt = barite, Cb = carbonate mineral, Dol = dolomite, Ep = epidote, Fl = fluorite, Lm = limonite, Mcld = magnesiochloritoid, Py = pyrite, Tpz = topaz (pyknite), Tr = tremolite, Qtz = quartz.

6.1.3. Hydrothermal breccia

Hydrothermal breccia is represented with Ž-5, Ž-6, Ž-7 and Ž-22 sample that appear in proximity of the deposit. This type of breccia, consisting of fluorite, barite and dolostone, makes approximately 20% of a deposit. Samples Ž-6, Ž-7 and Ž-22 consist predominantly out of fluorite and barite, besides smaller amounts of dolostone. In these three breccia samples fluorite and barite together, make 60 vol. % of them. On the other hand, sample Ž-5 consists mostly out of dolostone whereas fluorite, barite and quartz occupy minority of the sample. In this sample alone, fluorite and barite make approximately 20 vol. % of it. Macroscopically, barite is white in colour, has pearly lustre and is often present in shape of thin tabular crystals. Fluorite goes from colourless to intensively purple in colour and has vitreous lustre. Dolostone is dark grey in colour and relatively weathered to fresh.

The micropetrographical study illustrates the presence of barite, fluorite, dolomite and quartz in thin sections of all four samples of hydrothermal breccia. Barite and fluorite as main ore minerals. **Barite** is fine to coarse-grained, but also present as elongated or is occurring as fan-shaped aggregates. In Ž-6, Ž-7 and Ž-22 sample, barite occurs mostly as fan-shaped aggregates and is present in minority as fine-grained with anhedral to subhedral grain form. In Ž-5 sample barite is dominantly present as fine to coarse-grained with mineral grains exhibiting anhedral to subhedral grain form. It can be also found included in quartz or fluorite grains. Dimensions of barite mineral grains range from 0.02 to 4.50 mm. They have perfect to poor visible cleavage

with extinction parallel or symmetrical to cleavage. Interference colours vary from white to grey of I order. Barite mineral grains are fresh, often with sharp contact to other grains, but can show signs of alterations on the edges. Barite occupies ≈15 vol. % of four thin sections.

Fluorite is dominantly coarse-grained, isotropic and has anhedral grain form (**Fig. 6-2C**) in all four samples. Dimensions of fluorite mineral grains range from 0.05 to 5.50 mm. It has perfect to poor visible cleavage. The fluorite grains are sometimes intersected with thin veinlets filled with secondary carbonates. The contact of fluorite with other mineral grains is mostly sharp to irregular. Fluorite occupies from 2 to 70 vol. % of four thin sections.

Dolomite is present as fine-grained with anhedral grain form. Dolomite mineral grains show distinct change of relief and have poor to no visible cleavage. Extinction is parallel to cleavage (if present). Dimensions of dolomite grains vary from 0.02 to 0.36 mm. Dolomite occupies approximately 10 vol. % of four thin sections.

Quartz grains are fresh and have anhedral grain form with undulose extinction (**Fig. 6-2C**). Dimensions of quartz mineral grains range from 0.02 to 6.50 mm. Interference colour is white of I order. They can include smaller grains of barite with mostly sharp but also irregular contact with other mineral phases. Quartz occupies from 1 to 10 vol. % of four thin sections.

6.1.4. Ba-F vein type mineralization

Ba-F vein type mineralization is dominant type of mineralization in the Žune deposit present in most of the samples, excluding Ž-5, Ž-6, Ž-7 and Ž-22 sample. Veinlets containing barite and fluorite as main ore minerals are hosted in dolostone. These two mineral phases are dominant components followed with smaller amount of quartz. Thin limonite layer is characteristic on dolostone-veinlets contact. Thickness of these veinlets varies from 1.00 to 5.75 mm. In few observed hand specimens it could be seen that thicker veinlets show linear to sublinear alignment while in most of the other samples they do not show preferred orientation. Barite and fluorite show similar physical properties in this sample types as in those of hydrothermal breccia.

The micropetrographical study illustrates the presence veinlets in various shape, size and mineral association controlled by hydrothermal fluids. They can be subdivided into three types based on different mineral associations and thickness:

Type 1. Secondary carbonate-limonite veinlets: this type of veinlets is the thinnest of the three veinlet types. Their dimension is 0.07 mm or less and they are intersected by type 2 and type 3 veinlets.

Type 2. Secondary carbonate-quartz/fluorite-limonite veinlets: this type of veinlets appear similar to type 1 veinlets containing negligible amounts of quartz or fluorite. Thickness of veinlets ranges from 0.08 to 0.35 mm, and are intersected by type 3 veinlets.

Type 3. Barite-fluorite-quartz-pyrite veinlets: this type of veinlets is occurring in most of the thin sections (e.g. Ž-2, Ž-9, Ž-14, etc.). They vary in thickness from 0.36 to 5.75 mm. Contact between veinlets and dolomite is marked by presence of sulphides-pyrite that commonly alters to limonite.

Barite occurs fine to coarse-grained or is present as fan-shaped aggregates (**Fig. 6-2E**). Barite mineral grains have anhedral to subhedral grain form with its dimensions varying from 0.01 to 6.64 mm. They show perfect to poor visible cleavage with extinction parallel or symmetrical to cleavage. Interference colours vary from white to grey of I order. Some barite grains can contain fluorite, quartz and muscovite inclusions. Their contact to other mineral phases like fluorite and quartz is sharp, irregular. Signs of barite mineral grains weathering are observed. Barite occupies from 1 to 40 vol. % of thin section in this samples type.

Fluorite is fine to coarse-grained isotropic and has anhedral grain form. Dimensions of fluorite mineral grains range from 0.03 to 4.96 mm. It has perfect to poor visible cleavage. Thin veinlets filled with secondary carbonates commonly intersect fluorite grains. On their edges weathering consequences are seen with irregular contact to other mineral grains present. Fluorite occupies from 3 to 75 vol. % of thin section in this samples type.

Quartz grains are fresh with anhedral to subhedral grain form and have undulose extinction. Dimensions of quartz mineral grains range from 0.01 to 2.50 mm. Interference colour is white of I order. They are also found included within barite mineral grains with common irregular contact between them. Quartz occupies from 1 to 5 vol. % of thin section in this samples type.

6.2. Deposition succession

The mineralogy of the Žune deposit is relatively simple, with the main ore minerals being fluorite and barite. Other members of the Žune mineral assemblage are tremolite, Mg-chloritoid, topaz (pyknite), epidote, rutile and limonite. These remaining minerals have not been recognized in hand specimen, but only in the thin sections. Vein type mineralization is the dominant type of mineralization in the deposit with special emphasis put on determination of veinlet generations and mineral phases therein. Based on microscopic analysis it was determined that veinlets type 1 are the oldest of three due to being intersected by type 2 and type 3 veinlets. Type 1 veinlets predominantly consist of secondary carbonates with limonite occurring on their edges. Type 1 and type 2 veinlets consist of similar mineral phases but those of second type belong to younger generation containing negligible amount of quartz or fluorite. Furthermore, type 3 veinlets are the youngest of three types identified as they crosscut first two veinlet types. The veinlets of the youngest generation are composed out of barite and fluorite in greatest amount, followed by quartz and pyrite in smaller quantities. Thus, barite and fluorite in type 3 veinlets are deposited first, with quartz following. Pyrite, in concerned veinlet type, is occurring on dolomite-veinlet border. Alongside pyrite, chalcopyrite was detected by XRD, though not recognized in thin section. The relationship between sulphide minerals, fluorite and/or barite and quartz indicate near-simultaneous crystallization. A simplified paragenetic sequence of mineral phases in the Žune deposit is presented in **Figure 6-3**.

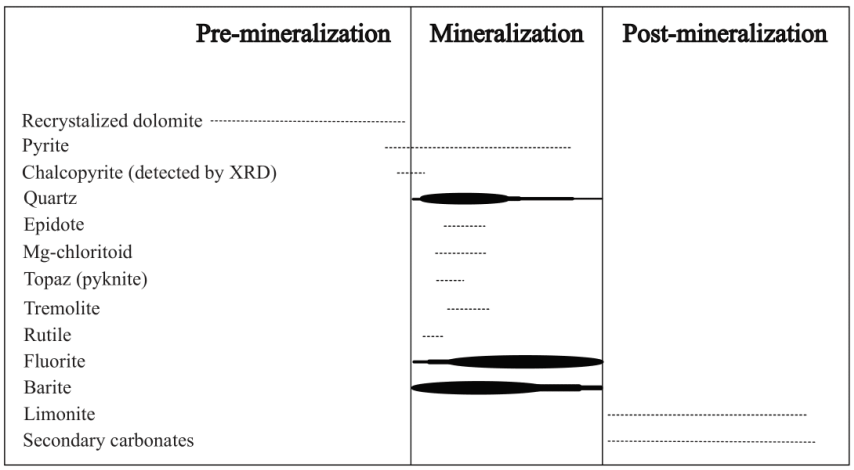

Figure 9-3. Simplified paragenetic sequence of minerals in the Žune deposit.

6.3. X-ray diffraction on selected ore sample

XRD analysis was conducted on Ž-5, Ž-7, Ž-16 and Ž-20 ore sample selected based on previous micropetrographical and geochemical analyses. Dominant mineral phases in Ž-5 sample, recognized on XRD-image are dolomite, calcite and fluorite. Occasionally, quartz and chloritoid mineral phases are observed (**Fig. 6-4**). The quantities of muscovit, barite, tremolite, pyknite, pyrite and limonite mineral phases weren't sufficient to register on a powder pattern. Ž-7 (**Fig. 6-5**), Ž-16 (**Fig. 6-6**) and Ž-20 (**Fig. 6-7**) samples are consisted out of barite, fluorite and quartz and occasional dolomite. In Ž-20 sample, small peaks of chalcopyrite were detected.

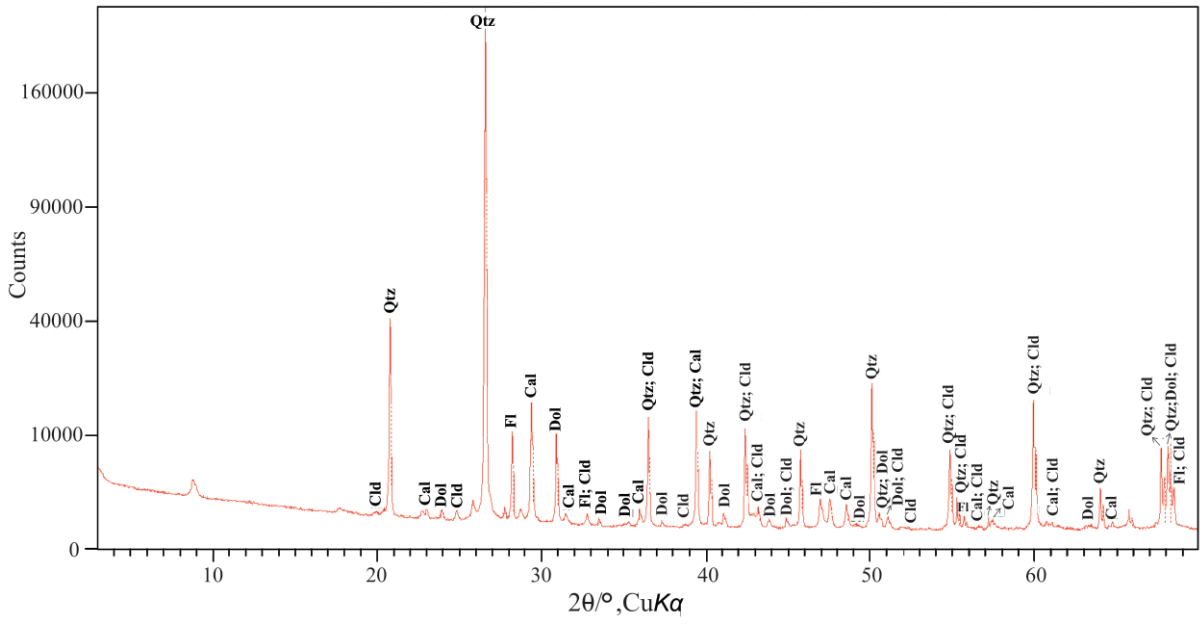

Figure 10-4. Result of XRD analysis for Ž-5 sample. (Dol = dolomite, Cal = calcite, Fl = fluorite, Qtz = quartz, Cld = chloritoid).

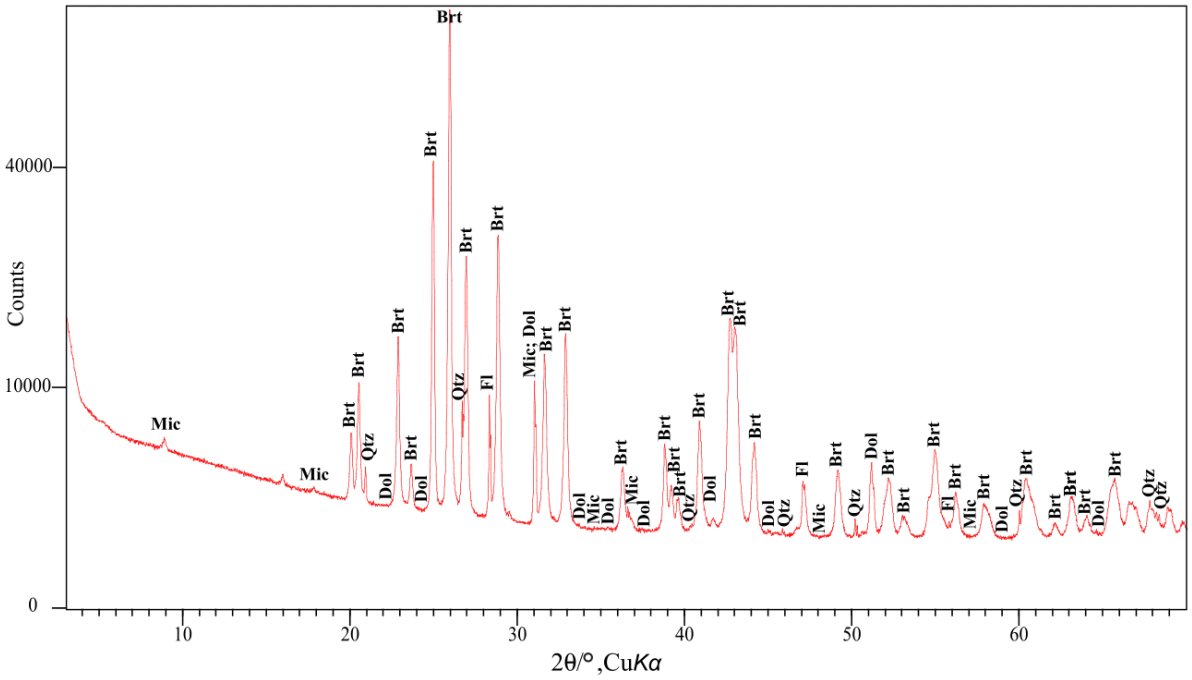

Figure 11-5. Result of XRD analysis for Ž-7 sample. (Brt = barite, Dol = dolomite, Fl = fluorite, Qtz = quartz, Mic = micas).

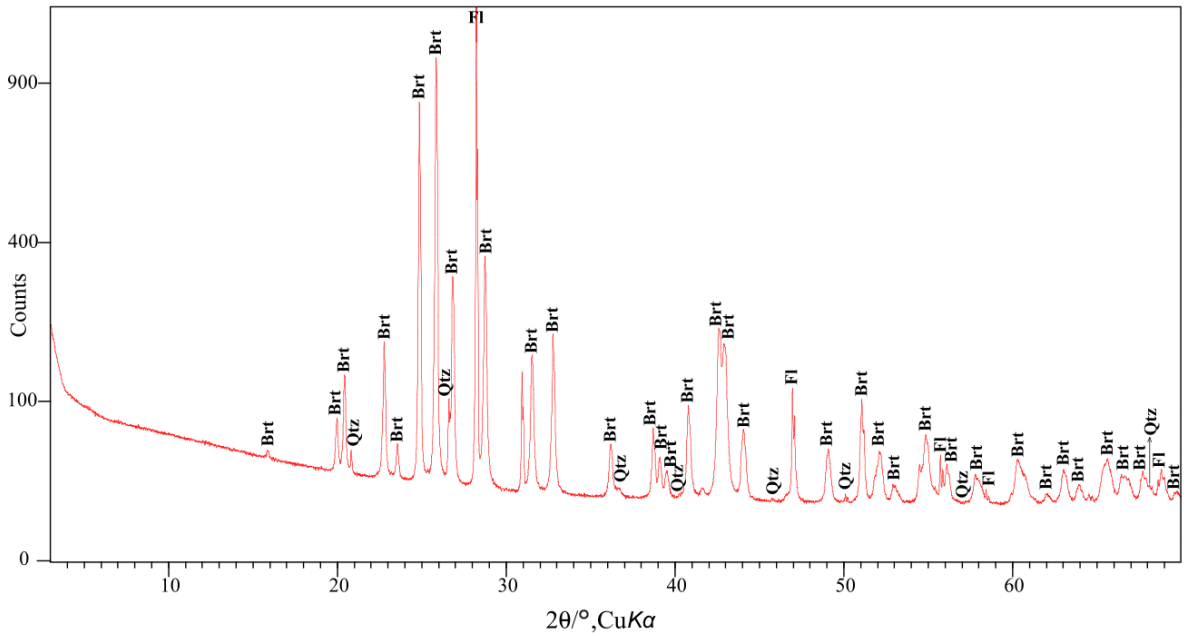

Figure 12-6. Result of XRD analysis for Ž-16 sample. (Brt = barite, Fl = fluorite, Qtz = quartz).

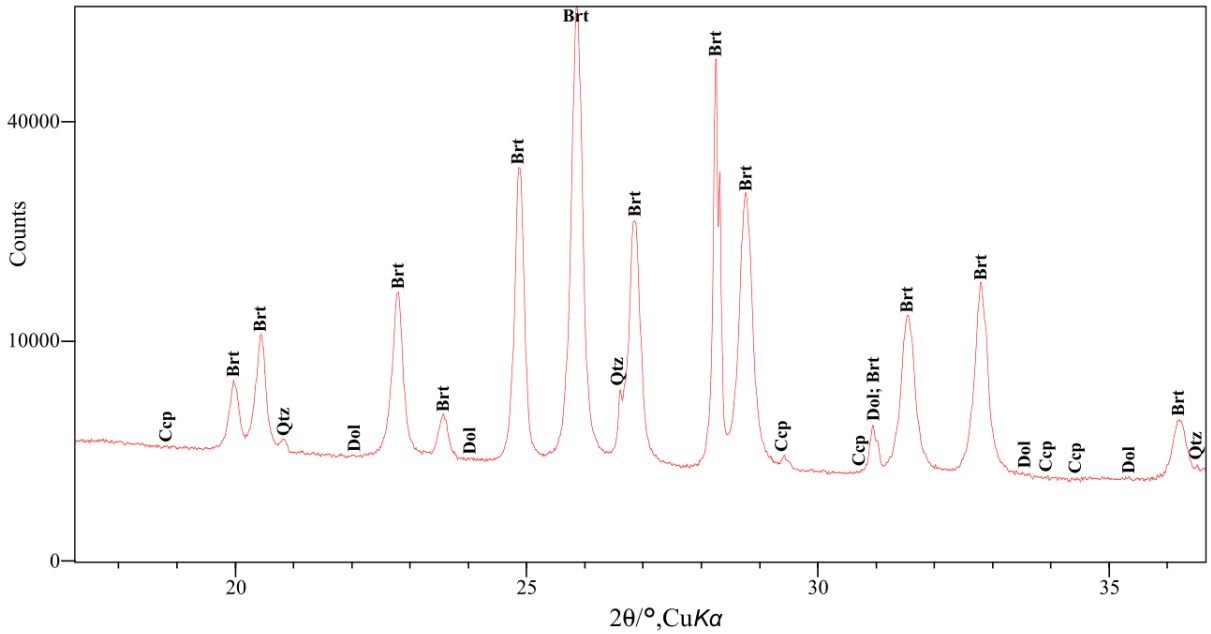

Figure 13-7. Result of XRD analysis for Ž-20 sample. (Brt = barite, Dol = dolomite, Qtz = quartz, Ccp = chalcopyrite).

6.4. The host rock and ore geochemistry

6.4.1. Macroelements

Geochemical analysis of the major element oxides, expressed in mass percentage, is shown in **Table 6-1**. The oxide composition of analysed dolostone Žune samples is mostly comprised of calcium oxide (CaO) and magnesium oxide (MgO). CaO varies from 30.24 to 32.38 mass. % while the content of MgO ranges from 15.62 to 17.35 mass. % with high loss of ignition (LOI) (43.61–45.58 mass. %). Except for SiO_2 (1.33–3.65 mass. %) and F (2.55–3.65 mass. %) present in significant contents, other major element oxides are present in the dolostone samples in trace amounts. The samples of Ba-F vein type mineralization are composed predominantly of CaO (6.30–66.03 mass. %) and barium oxide, BaO (3.92–50.23 mass. %) with appreciable concentrations of SO_3 (2.05–26.22 mass. %) and fluor (2.01–22.88 mass. %). Positive correlation between BaO and SO_3, as well as for CaO and fluor, is present. From other major element oxides only SiO_2 is present in significant values ranging between 2.92 and 5.77 mass. % with LOI varying from 0.30 to 3.12 mass. %.

Table 6-2. Oxide composition of analysed samples. All values given in mass. %.

Sample type	Dolostone					Ba-F vein type mineralization					Hydrothermal breccia	
Sample	**Ž-1**	**Ž-2**	**Ž-4**	**Ž-10**	**Ž-17**	**Ž-3**	**Ž-11**	**Ž-16**	**Ž-19**	**Ž-20**	**Ž-7**	**Ž-Comp**
SiO_2	2.20	2.06	1.33	1.74	3.65	5.77	2.92	3.28	4.29	3.90	5.53	5.31
TiO_2	0.03	0.02	0.02	0.01	0.02	<0.01	<0.01	<0.01	<0.01	<0.01	0.01	0.01
Al_2O_3	0.74	0.37	0.38	0.27	0.32	0.35	0.38	0.09	0.30	0.16	0.24	0.32
Fe_2O_3	0.85	0.75	0.78	0.87	0.75	0.30	0.07	0.09	0.04	0.15	0.17	0.81
Cr_2O_3	<0.01	<0.01	<0.01	<0.01	<0.01	<0.01	<0.01	<0.01	<0.01	<0.01	<0.01	<0.01
MgO	17.14	17.35	16.47	16.48	15.62	0.78	0.02	0.10	0.17	0.37	0.55	5.75
MnO	0.11	0.11	0.10	0.11	0.10	0.01	<0.01	<0.01	<0.01	<0.01	<0.01	0.06
CaO	31.96	32.38	31.15	30.24	30.81	49.06	65.10	7.98	66.03	6.30	1.71	28.61
K_2O	0.15	0.06	0.06	0.05	0.04	0.06	0.05	0.02	0.04	0.03	0.05	0.06
Na_2O	0.06	0.06	0.07	0.05	0.06	0.17	0.26	0.05	0.25	0.05	0.02	0.09
P_2O_5	0.02	<0.01	<0.01	<0.01	<0.01	<0.01	<0.01	<0.01	0.02	<0.01	<0.01	<0.01
BaO	0.28	0.83	0.02	0.51	0.39	15.93	5.68	49.05	3.92	50.23	50.74	23.35
SrO	<0.01	0.01	<0.01	0.01	<0.01	0.23	0.08	1.26	0.12	1.17	1.26	0.52
SO_3 *	0.15	0.43	0.01	0.27	0.20	8.32	2.97	25.61	2.05	26.22	26.49	12.19
F *	2.83	2.87	2.87	2.55	3.16	16.68	22.63	2.73	22.88	2.01	0.33	7.36 **
LOI	45.22	45.18	45.58	44.6	43.61	3.12	0.30	1.28	0.44	0.90	0.95	13.39
Total	101.73	102.49	98.84	97.75	98.74	100.78	100.45	91.53	100.54	91.50	88.05	97.83

6.4.2. Microelements

Samples show microelement concentrations mostly lower than the average composition of the upper crust (**Fig. 6-8**). Elemental composition of analysed samples expressed in ppm is shown in **Table 6-2**. The exception is Ba that is elevated in all analysed samples, excluding Ž-4, with highest concentration in Ž-11 sample (8391 ppm), Sr in Ž-7 (2256 ppm), Ž-16 (3030.10 ppm) and Ž-20 (2771.20 ppm) and Y that is slightly elevated in Ž-3, Ž-11 (highest concentration of 41 ppm) and Ž-19 sample. There is strong positive correlation between elevated concentrations of Ba and Sr with barite quantities in the samples. Increased concentration of Y could be linked with occurrence of fluorite in the samples.

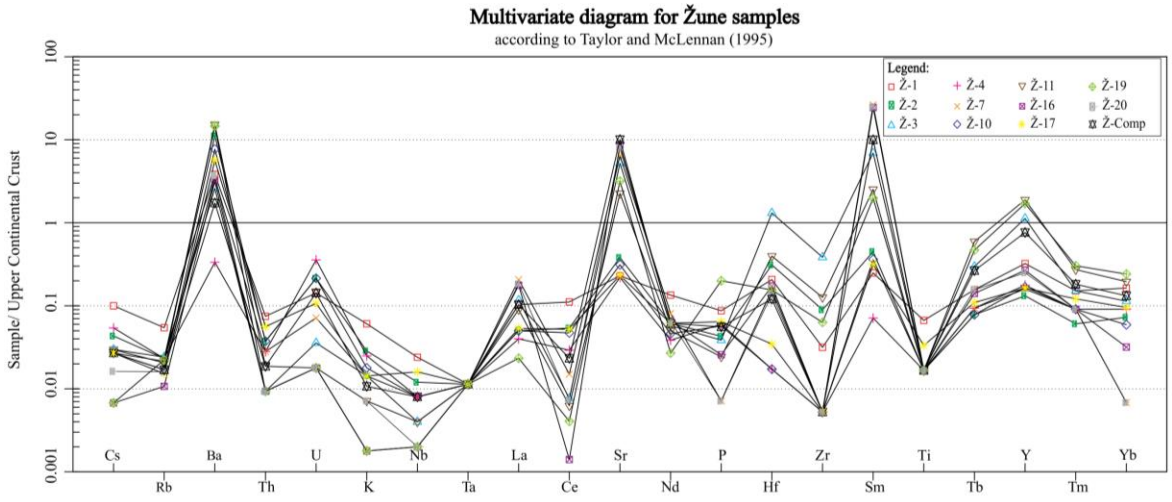

Figure 14-8. Upper Continental Crust normalized (**Taylor and McLennan, 1995**) trace element distribution in analysed samples.

The REE spectra, normalized to the average values for chondrites (**Anders and Grevesse, 1989**), are shown in **Figure 6-9**. Rare earth element concentrations are shown in **Table 6-3**. The ΣREE varies from 5.73 to 166.01 ppm in analysed samples. The enrichment of light REEs in regard to heavy REEs is visible in most of the samples. Ratio ΣLREE/ΣHREE is highly uneven with ΣLREE going up to 598.13 ppm while ΣHREE up to 24.42 ppm. As observed in **Fig. 6-9**, higher concentrations of LREEs are detected, with strong positive europium (Eu) and samarium (Sm) anomalies.

Table 6-3. Elemental composition of analysed samples. All values given in ppm.

S. type	Dolostone					Ba-F vein type mineralization					H.breccia	
Sample	**Ž-1**	**Ž-2**	**Ž-4**	**Ž-10**	**Ž-17**	**Ž-3**	**Ž-11**	**Ž-16**	**Ž-19**	**Ž-20**	**Ž-7**	**Ž-Comp**
Ba	2110	6126	184	4238	3107	1426	8391	1739	8044	2040	1889	953
Be	0.28	0.14	0.17	0.27	0.33	0.14	0.10	0.13	0.79	0.06	<0.05	0.35
Co	0.40	0.40	0.60	0.90	0.50	0.90	1.50	0.50	0.20	1.00	3.40	3.70
Cs	0.32	0.10	0.14	0.07	0.07	0.09	0.10	0.04	0.07	0.05	0.08	0.10
Ga	1.80	1.20	1.10	1.10	0.80	0.70	0.50	0.20	0.40	0.30	0.70	0.70
Hf	1.20	1.80	<0.20	<0.20	0.20	7.60	2.30	1.00	0.90	0.80	0.90	0.70
Nb	0.60	0.30	0.20	0.20	0.40	0.10	0.10	<0.10	<0.10	<0.10	0.20	0.20
Rb	6.10	2.60	2.60	1.90	1.70	2.70	2.30	1.20	2.50	1.80	2.40	1.90
Sn	0.30	<0.20	<0.20	<0.20	0.20	<0.20	<0.20	<0.20	<0.20	<0.20	0.50	0.50
Sr	64.80	111.20	61.70	120.40	99.60	1862.50	635.50	>10000	999.4	9248.50	>10000	4116
Ta	<0.10	<0.10	<0.10	<0.10	0.20	3.00	2.20	0.80	1.90	0.50	0.20	0.90
Sc	0.80	0.50	0.40	0.50	0.60	0.30	0.10	<0.10	<0.10	<0.10	0.10	0.40
Th	0.67	0.45	0.16	0.14	0.33	0.68	0.46	<0.05	0.30	<0.05	<0.05	0.09
U	0.39	0.53	0.94	0.61	0.30	0.22	0.17	<0.05	0.07	0.07	0.17	0.34
V	<10.00	<10.00	96.00	<10.00	20.00	122.00	56.00	<10.00	23.00	<10.00	<10.00	11.00
W	1.00	<1.00	2.00	2.00	1.00	4.00	2.00	2.00	2.00	2.00	1.00	2.00
Zr	6.00	17.00	<2.00	<2.00	<2.00	73.00	73.00	<2.00	12.00	<2.00	<2.00	<2.00
Y	7.10	2.90	3.90	3.70	3.60	24.80	41.60	5.90	37.50	5.50	3.50	16.80
Mo	0.10	0.13	0.07	0.09	0.09	0.09	<0.05	0.08	0.09	0.05	0.06	0.18
Cu	12.80	8.00	13.00	4.70	2.40	3.40	4.10	2.60	1.50	6.40	7.60	8.70
Pb	2.30	2.00	2.30	3.70	3.90	3.50	4.40	2.70	6.70	8.40	5.20	6.80
Zn	6.00	6.00	5.00	7.00	5.00	3.00	<2.00	<2.00	<2.00	<2.00	2.00	7.00
Ni	65.90	89.20	81.30	102.90	34.80	33.80	25.50	57.20	74.70	24.00	33.10	56.58
As	91.70	156.20	9.50	5.00	0.40	8.80	2.40	2.50	2.70	3.20	4.50	15.70
Cd	<0.02	0.03	<0.02	0.04	<0.02	0.02	0.02	0.03	<0.02	<0.02	0.02	0.05
Sb	7.40	2.40	1.60	2.50	2.10	0.90	0.80	0.80	<0.50	2.00	1.80	6.20
Bi	0.01	0.01	0.02	0.02	<0.01	0.01	0.01	0.01	<0.01	<0.01	0.08	0.02
Ag	0.11	0.06	0.05	0.03	0.02	0.02	0.02	0.02	0.02	0.03	0.06	0.08
Tl	0.29	0.22	0.05	0.03	<0.02	0.03	<0.02	<0.02	<0.02	<0.02	0.02	0.06
Se	<1.00	<1.00	<1.00	<1.00	<1.00	<1.00	<1.00	<1.00	<1.00	<1.00	<1.00	<1.00

Ž-7, Ž-16 and Ž-20 samples show the most deviating positive Eu and Sm anomalies with Eu concentrations ranging between 40.73 and 43.52 ppm and Sm between 110.12 and 118.28 ppm. The Eu/Eu* ration for these three samples is 24.27; 20.28 and 20.89, respectively. The Eu anomaly was calculated as Eu/Eu*= EuN/√[(SmN)*(GdN)]. Other significant anomalies observed in **Figure 6-9** are negative cerium (Ce) and ytterbium (Yb) anomalies. REEs and microelements show similar behaviour patterns in most of the samples. Exceptions are Ž-1 and Ž-4 samples as they exhibit no distinctive anomalies or trends, but equal and slightly increased concentrations of all REEs.

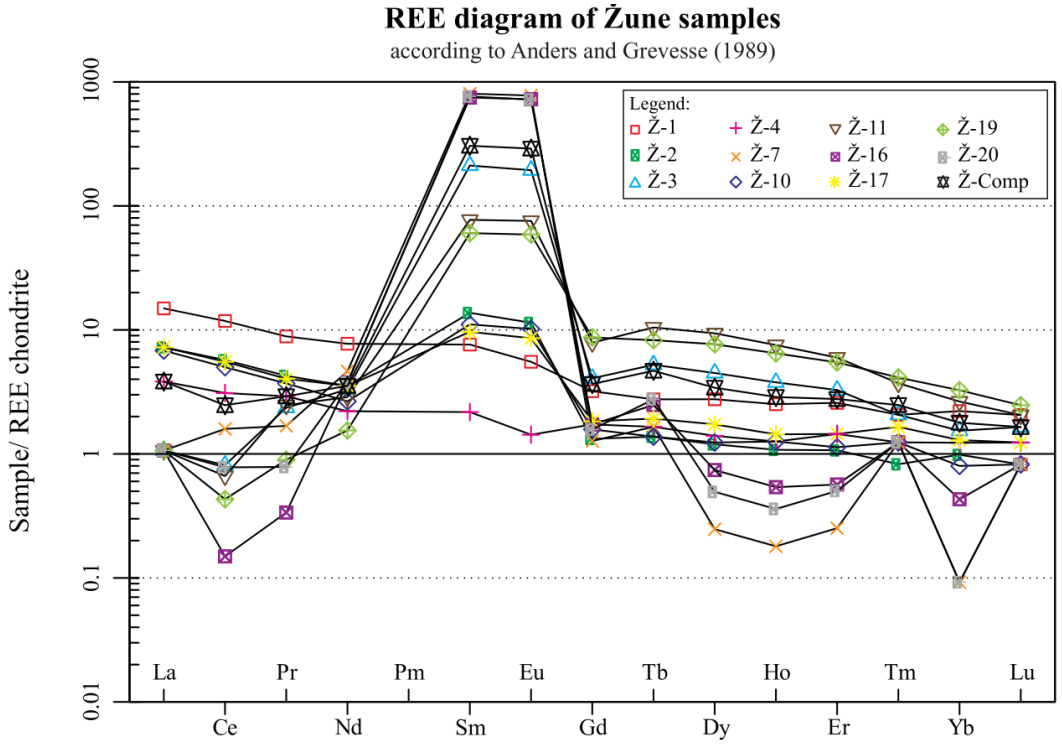

Figure 15-9. Chondrite normalized (**Anders and Grevesse, 1989**) REE distribution in analysed samples of the Žune deposit.

Hierarchical cluster analysis (HCA) was conducted in order to establish the correlation between geochemical contents of major element oxides and microelements. The visual observation of constructed dendrogram is main principle based on which samples and variables were classified in HCA. This analysis resulted in one dendrogram of analysed samples where three geochemically different cluster can be recognized (**Fig. 7-1**). First cluster is Al_2O_3 and Fe_2O_3 together with MgO and certain REEs (La, Ce and Pr). BaO and SiO_2 make second cluster with

Sr, Sm and Eu while third cluster is CaO and Na_2O one, grouped with F, Y and other REEs. A detailed examination reveals linkage of second and third cluster at an elevated distance where they are further connected with first cluster.

Table 6-4. Rare earth element composition of analysed samples. All values given in ppm.

Sample type	Dolostone					Ba-F vein type mineralization					Hydrothermal breccia	
Sample	**Ž-1**	**Ž-2**	**Ž-4**	**Ž-10**	**Ž-17**	**Ž-3**	**Ž-11**	**Ž-16**	**Ž-19**	**Ž-20**	**Ž-7**	**Ž-Comp**
La	3.50	1.70	0.90	1.60	2.45	0.50	0.50	0.50	0.50	0.50	0.50	0.90
Ce	7.12	3.45	1.87	3.02	3.34	0.49	0.40	0.09	0.26	0.47	0.96	1.49
Pr	0.79	0.38	0.26	0.33	0.36	0.21	0.22	0.03	0.08	0.07	0.15	0.26
Nd	3.50	1.60	1.00	1.20	1.60	1.50	1.30	1.70	0.70	1.70	2.10	1.60
Sm	1.12	2.02	0.32	1.63	1.42	31.14	11.36	110.12	8.88	112.27	118.28	44.93
Eu	0.31	0.64	0.08	0.57	0.48	10.87	4.24	40.59	3.29	40.33	43.52	16.23
Gd	0.63	0.26	0.34	0.31	0.36	0.80	1.55	0.34	1.71	0.31	0.25	0.72
Tb	0.10	0.05	0.06	0.05	0.07	0.19	0.38	0.09	0.30	0.10	0.06	0.17
Dy	0.67	0.29	0.34	0.30	0.42	1.09	2.28	0.18	1.86	0.12	0.06	0.83
Ho	0.14	0.06	0.07	0.07	0.08	0.21	0.42	0.03	0.36	0.02	0.01	0.16
Er	0.41	0.17	0.23	0.18	0.23	0.52	0.95	0.09	0.87	0.08	0.04	0.44
Tm	0.05	0.02	0.03	0.03	0.04	0.05	0.09	0.03	0.10	0.03	0.03	0.06
Yb	0.36	0.16	0.20	0.13	0.21	0.25	0.43	0.07	0.53	0.03	0.03	0.29
Lu	0.05	0.02	0.03	0.02	0.03	0.04	0.05	0.02	0.06	0.02	0.02	0.04
ΣREE	18.75	10.82	5.73	9.44	10.34	47.86	24.17	153.88	19.50	156.05	166.01	68.12
Eu/Eu*	1.13	2.71	0.73	2.45	2.05	6.66	3.09	20.28	2.58	20.89	24.47	8.73

7. Discussion

7.1. Ore deposition conditions

Contact zone mineralogy

Particular importance in this chapter is put on tremolite, magnesiochloritoid, pyknite (topaz) and epidote among other primary accessory minerals in the mineral assemblage, as they indicate specific forming conditions of the deposit.

Tremolite [$Ca_2Mg_5Si_8O_{22}(OH)_2$] is present in the minority of the samples in the Žune deposit (Ž-4, Ž-5, Ž-17 and Ž-19), occurring predominantly on the fluorite-quartz-secondary carbonate contact. The quartz presence in assemblage indicates that tremolite-forming reaction did not went to completion. Several studies (**Slaughter et al., 1975**; **Eggert and Kerrick, 1981**; **Cook and Bowman, 2000**) suggest that, accordingly to Žune mineral paragenesis, tremolite was most likely formed by the reaction:

$$\underset{\text{(dolomite)}}{5CaMg(CO_3)_2} + \underset{\text{(quartz)}}{8SiO_2} + H_2O = \underset{\text{(tremolite)}}{Ca_2Mg_5Si_8O_{22}(OH)_2} + \underset{\text{(calcite)}}{3CaCO_3} + 7CO_2, \qquad (7\text{-}1)$$

with pressure of 2 kbars, temperature at 484°C +/- 15°C and X_{CO2}= 0.85, as the corresponding equilibrium conditions. **Slaughter et al.** (**1975**) provided these data as starting points for the thermodynamic calculation of phase equilibria in $CaO\text{-}MgO\text{-}SiO_2\text{-}H_2O\text{-}CO_2$ system. Reaction involving talc, mentioned in previous studies (**Slaughter et al., 1975**; **Cook and Bowman, 2000**), can be excluded so far since no talc was found in carbonates of the Žune deposit. The rare assemblage Tremolite + Dolomite reflects either local mineralogical (and hence compositional) zoning on a larger scale than of a thin section, or local metasomatism (**Cook and Bowman, 2000**). In a zone with tremolite-bearing dolomites, the low temperature limit for tremolite matches with the upper limit for talc at approximately 450°C according to **Bucher and Frey** (**2002**).

Chloritoid group has the general formula $(Fe^{2+},Mg,Mn^{2+})_2(Al,Fe^{3+},Cr^{3+},Ga)Al_3O_2[(Si,Ge)O_4]_2(OH)_4$ with monoclinic and triclinic polytypes (**Chopin et al, 1992** and reference therein). **Magnesiochloritoid** [$MgAl_2(SiO_4)O(OH)_2$] is an Mg-end-member of chloritoid that characteristically occurs in high pressure terrains and is often called “stress” mineral, but

according to **Deer et al.** (**1997**) it is also found in quartz-carbonate veins and other hydrothermal environment. In the Žune deposit it is present in three samples (Ž-5, Ž-17 and Ž-19) incorporated within quartz. Mg-chloritoid forming reaction is suggested by **Ghent et al.** (**1989**):

$$\underset{\text{(chlorite)}}{(Mg,Fe^{2+})_5Al(Si_3Al)O_{10}(OH)_8} + \underset{\text{(calcite)}}{4CaCO_3} + 4CO_2 = \underset{\text{(dolomite)}}{4CaMg(CO_3)_2} + \underset{\text{(quartz)}}{2SiO_2} + \underset{\text{(Mg-chloritoid)}}{MgAl_2(SiO_4)O(OH)_2}. \quad (7\text{-}2)$$

Reaction was proceeded with chlorite component-clinochlore that involves in reaction with calcite and results in formation of Mg-chloritoid, dolomite and quartz. The presence of chlorite lacks in the mineral assemblage, similar as in **Ghent et al.** (**1989**), with strong possibility of occurring in minor quantities but, due to smaller number of thin sections observed it was not detected. Forming conditions for reaction (7-2) were, constant total pressure of 5 kbars for part of the K_2O-Na_2O-FeO-MgO-CaO-Al_2O_3-SiO-H_2O-CO_2 system and X_{CO2} exceeding ≈ 0.01 at 350°C. In a series of mineral forming reaction, **Livi et al.** (**2002**) stated that mineral assemblage Calcite + Dolomite + Chloritoid is present at pressure of 2 kbars with temperature range from 320°C to 400°C.

Pyknite [$Al_2(SiO_4)(F,OH)_2$] occurs in three samples (Ž-5, Ž-17 and Ž-19) in the Žune deposit commonly included in quartz mineral grains. At low Ca^{2+}/H^+ activity ratios topaz is stable phase whereas fluorite is deposited at high Ca^{2+}/H^+ ion activity ratios (as referenced in **Srivastava and Sukhchain, 2005**). **Wright and Kwak** (**1989**) stated that under conditions of very high F-activity topaz can be formed as a result of the instability of muscovite in the presence of HF. The following reaction may be responsible for the pyknite forming, according to **Wright and Kwak** (**1989**):

$$\underset{\text{(muscovite)}}{K_2Al_2(Si_6Al_2O_{20})(OH)_4} + 3HF + 2H^+ = \underset{\text{(topaz)}}{3Al_2(SiO_4)(OH,F)_2} + \underset{\text{(quartz)}}{3SiO_2} + 2K^+ + 4H_2O. \quad (7\text{-}3)$$

Thomas (**1994**) studied different types of topaz in Erzgebirge area, Germany, where he reported forming temperatures of hydrothermal topaz at ≤ 330°C with fluorine content (in F/(F + OH) molar ration) ≤ 0.76.

Epidote [$Ca_2(Al_2,Fe3^+)(Si_2O_7)(SiO_4)O(OH)$] is mostly present in granular aggregates, occurring in four samples (Ž-2, Ž-9, Ž-15 and Ž-17) in the Žune deposit. In lower-pressure hydrothermal environments, epidote is common mineral in skarns, in propylitic altered volcanic rocks and in late-stage veins related to silicic intrusions (**Bird and Spieler, 2004** and reference therein). Same authors described formation of epidote by precipitation in cavities and by replacements of silicates, carbonates and Fe-oxides. **Arnason et al.** (**1993**) presented epidote-forming reaction:

$$6Ca_2FeAI_2Si_3O_{12}(OH) + 4CO_2 = 4Ca_2AI_3Si_3O_{12}(OH) + 3Fe_2O_3 + 4CaCO_3 + 6SiO_2 + H_2O, \quad (7\text{-}4)$$

(epidote-ss) (epidote-ss) (hematite) (calcite) (quartz)

under low temperature (200-400°C) and low pressure (< 5 kbars) conditions. Limonite is recognized is analysed samples but it is possible that hematite occurs is small amounts matching the Fe_2O_3 content in **Table 6-1**. The reaction (7-4) with concerned assemblage, a vein assemblage in Salton Sea geothermal system, is exothermic with Al^{3+} content of epidote decreasing with increasing temperature. Epidote + Hematite + Calcite + Quartz assemblage is common in Salton Sea geothermal system as reported by **Caruso et al.** (**1988**). Quantitative evaluation of physical and chemical variables based on epidote-ss composition may be unreliable due to sensitivity of epidote solid solutions to slight changes in fluid chemistry as stated in **Arnason et al.** (**1993**). Thus, it must be taken into consideration that under hydrothermal conditions, epidote is stable over a range of temperature and pressure (as referenced in **Bird and Spieler, 2004**).

Previous p/T estimation

As a part of the Ljubija ore field, forming conditions of the Žune deposit were one of the subjects' matter in **Palinkaš et al.** (**2016**). Few theories have been proposed about Ljubija ore deposits formation with **Palinkaš et al.** (**2016**) clarifying complex views on the origin of the mineralization. Same authors stated that thermal events in the Alpine Wilson cycle stage of the Permian early intra-continental rifting were in response to the high heat flow caused by thermal doming and thinning of the continental crust. Thus generating numerous hydrothermal cells in the thick piles of the post-Variscan overstep successions. This stage of the cycle produced hydrothermal deposits, including Ljubija ones as *loci typici* of the siderite-barite-polysulfide

deposits within Inner Dinarides, Gemerides and Eastern Alps. One of those deposits was Žune, where boiling of the ore forming fluids was recognised. **Jeremić** (**1958**) reported elements of hydraulic fracturing that structure and texture of the vein bear as important prerequisite for boiling of the hydrothermal fluid. Microthermometric measurements, Laser Raman spectroscopy and bulk crush-leak analysis by ionic chromatography were performed by **Palinkaš et al.** (**2016**) on fluorite and barite samples from the Žune deposit, with aim to investigate and confirm forming conditions mentioned above. Study of fluid inclusions in fluorite from fluorite-barite vein of the Žune deposit revealed nine different types of inclusions. The method was performed on liquid rich and vapour rich inclusions with or without daughter minerals. Investigation resulted with homogenization temperatures in range from 125° to 245°C for liquid rich inclusion of high salinity and vapour rich inclusions with very low salinity. Finding of numerous inclusions in one single crystal proved a requirement for multistage episodes of boiling under changeable pressure. Laser Raman spectroscopy was also performed on fluid inclusions from fluorite characterized as aqueous, liquid-rich containing halite daughter minerals with high salinity. As a result, aqueous liquid and aqueous gas and/or traces of CO_2 at room temperature were detected with no other volatiles present. Bulk-crush-leach analysis revealed maximum values of SO_4^{2-} up to 3 wt. % (or 30000 ppm) that were detected within single fluorite sample, explained as a consequence of contamination due to presence of barite solid inclusions. Research by **Palinkaš et al.** (**2016**) resulted in concluding that ore forming $NaCl\text{-}CaCl_2\text{-}H_2O$ fluids were highly variable in salinity with boiling phenomena contributed to the variability. The homogenization temperatures (T_h) were estimated between 100° and 310°C. The homogenization temperature of fluid inclusions is known to be the minimum temperature of the mineral formation (**Safina et al., 2021** and reference therein). Hydrothermal fluids were recognized as a mixture of high temperature-high salinity Permian evaporitic sea water, diluted by low-temperature-low-salinity sea or meteoric waters. The boiling temperature was controlled by hydrostatic pressure, same as variable depths of formation around 100-200 m below the land surface.

7.2. Hierarchical cluster analysis of the geochemical data

Distribution patterns of macro- and microelements as well as REEs were analysed in the Žune samples (Ž-1, Ž-2, Ž-3, Ž-4, Ž-7, Ž-10, Ž-11, Ž-16, Ž-17, Ž-19 and Ž-20) with aim to determine

geochemical and genetic connection among them. Determination of the relationship between macro-, micro- and REEs was based on two main approaches: plotting of the micro- and rare earth elements, and hierarchical clustering analysis. The HCA (**Fig. 7-1**) was performed in order to observe how major oxides are correlated with selected microelements and REEs in the analysed samples.

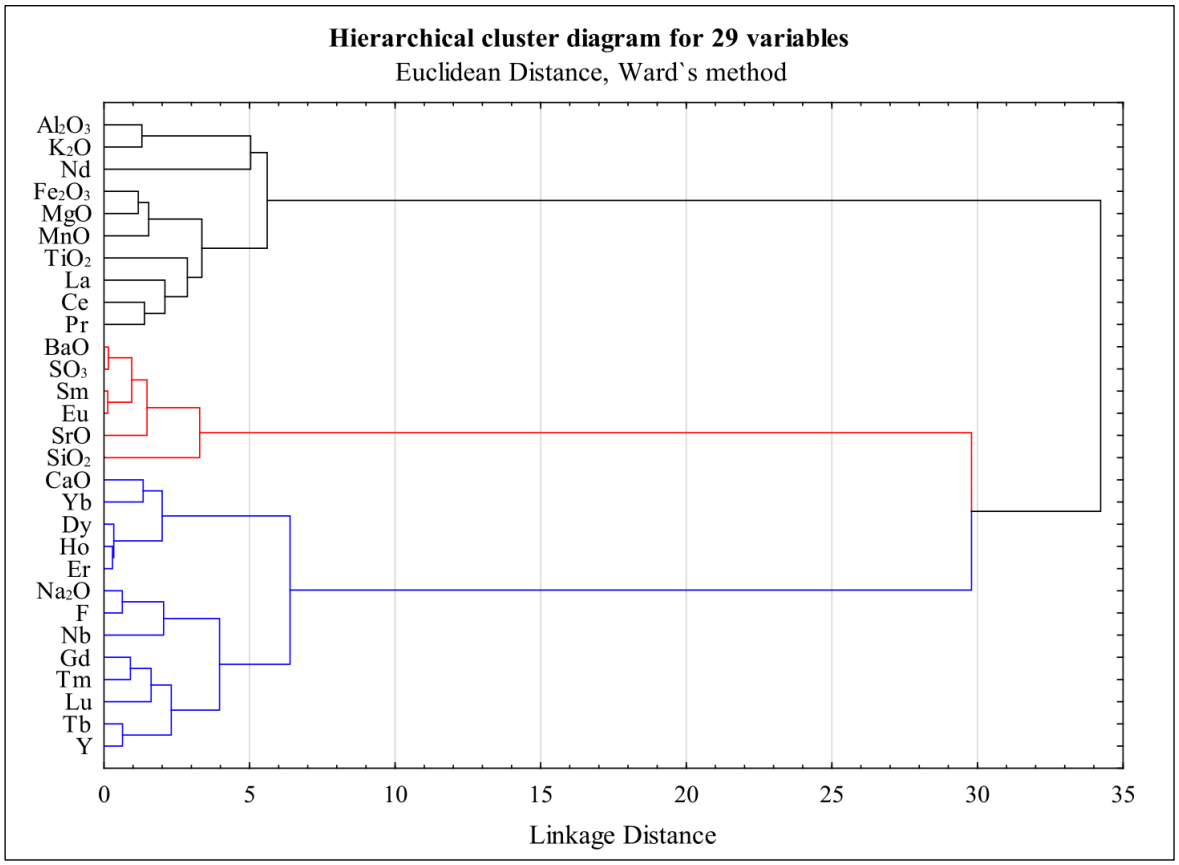

Figure 16-1. Hierarchical cluster analysis of the Žune samples

Dolostone

As far as dolostone geochemistry is concerned, Mn and Ni exhibit the most deviating behaviour patterns compared to the other elements. When compared Mn as MnO, alongside Ni, and Mg as MgO, a positive correlation appears between those two elements (Mn and Ni) with MgO. Though, stronger correlation is present between MnO and MgO (99.26%; **Table 7-1**) than between Ni and MgO (59.32%), there is a clear indication that substitution of ions in dolomite crystal structure has occurred. Mn substitutions are the most favourable at Mg site in crystal

lattice of dolomite with preference for this kind of substitution (Mn-Mg) as stated in **Austen et al.** (**2005**). The authors also presented Cd substitutions, alongside Mn ones, in dolomite but Cd was not detected so it is not important for this study. Furthermore, due to their similar ionic radii **Austen et al.** (**2005**) demonstrated there is a stabilization for substitution of Mg (ionic radius of 0.72 Å) sites for Ni (ionic radius of 0.69 Å). Though, an Mg-Mn substitution is more likely to have occurred as confirmed by their stronger correlation, it must be taken into consideration that Ni occupied some Mg sites in dolomite structure as impurity. The constructed dendrogram (**Fig. 7-1**) shows MgO and MnO clustering together and further connecting with other major oxides and REEs. To confirm mentioned above, a positive correlation is present between the content of dolomite with Mn and Ni concentrations in the sample, particularly in Ž-1, Ž-2 and Ž-10.

Barite impact

Comparative analysis of the trace element concentrations revealed that there is an obvious relationship between the Sr concentrations and the barite mineral phase in the samples. Thus, the highest concentrations of Sr occur in the samples containing the largest amount of barite (e.g. Ž-7, Ž-19 and Ž-20 sample). Also, a strong positive correlation amid strontium and barite is present implying that Sr is enriched in barite. This enrichment can be explained by the substitution of Ba^{2+} with Sr^{2+} in the barite crystal lattice as they have relatively similar ionic radii (Ba= 1.42 Å; Sr= 1.26 Å), and expressed as $SrSO_4$ component. Barite is usually rich in strontium and poor in rubidium (**Zou et al., 2016**). Strontianite ($SrCO_3$) as an individual phase was not detected in barite which was confirmed by XRD analysis conducted on samples Ž-7, Ž-16 and Ž-20. Similar case was noticed by **Jurković et al.** (**2010**) where X-ray analysis of barites demonstrated that strontianite did not exist as an individual phase within, though also having high content of Sr present in concerned mineral phase. **Jurković et al.** (**2010**) stated that such a relatively high Sr content is typical for an ascending hydrothermal type of mineralization, whereas a low content characterizes the volcano-sedimentary type of barite deposit. In addition, **Jurković et al.** (**2010**) exhibited the relationship between the $SrSO_4$ components in barites of Bosnia to other worldwide known barite deposits. They found that, as Brixlegg deposit in Austria and the Rudnany deposit in Slovakia, the barites of Bosnia are characterized by significantly higher $SrSO_4$ contents typical for hydrothermal epigenetic deposits. This was

explained as a consequence of the partial remobilization processes during Hercynian and Alpine orogeny.

The REE spectra of epithermal Žune deposit is mostly chondrite-like with shallow slopes, however, a disorder from that distribution pattern can be seen in Sm and Eu anomalies that are mildly positive for most of the samples and deviating in Ž-7, Ž-16 and Ž-20 sample (**Fig. 6-9**). It was also observed that higher concentrations of Sm and Eu follow higher quantities of barite in the samples which directs us to enrichment of these two light REEs in barite. This can be confirmed by the negative correlation of Sm and Eu with CaO and MgO (**Table 7-1**) meaning there is no Sm-Eu enrichment present in dolostone nor fluorite. This trend is most probably caused by ore-forming hydrothermal fluids rich in Sm and Eu, which presumably embedded in barite. Several studies (**Hajalilou et al, 2014**; **Volkov et al., 2021** and reference there in) stated that Eu, alongside Ce, anomaly is considered to be the marker of oxidation-reduction potential of the ore formation environment. Hence, the positive Eu anomaly can be caused due to reductive conditions that changes Eu^{3+} valent state to Eu^{2+} (**Hajalilou et al, 2014**). The authors (**Hajalilou et al, 2014**) also presented that if the ore-forming fluid is the final stage of the magmatic differentiation, the late fluid is enriched in Eu, K, Ba and Sr, where Eu^{2+} and Sr^{2+} are similar to Ba^{2+} that leads to their involvement in barite structure. Moreover, **Bau & Möller** (**1992**) (as referenced in **Safina et al., 2021**) suggested that positive Eu anomaly could indicate high temperature of mineral formation, >250°C, with reducing conditions and presence of the Eu^{2+} in mineralizing fluid. On the other hand, **Morgan et al.** (**1980**) presented an opinion that the positive Eu anomaly is related to the large radius of Eu^{2+} cations. The incorporation of REE ions in the barite structure will be more easily the bigger they are, as a consequence of large Ba^{2+} ionic radius (1.50 Å stated by **Morgan et al., 1980**, but 1.42 Å by renewed data). The Eu^{2+} ion is very similar in size and charge to Sr^{2+} (1.33 Å in VIII co-ordination) and is less difficult to accommodate in the barite structure than the smaller trivalent REEs. Additionally, the Eu^{2+} requires no charge compensation unlike Eu^{3+}. Based on renewed data the ionic radius of the Eu^{2+} is 1.25 and Sr^{2+} is 1.26 in VIII co-ordination. So according to **Morgan et al.** (**1980**), minerals that have large major ions like Ba^{2+} favour the replacement by the largest, hence lightest, REE ions such as Eu and Sm. In the constructed dendrogram it is observed that Sm and Eu make one small cluster that is connected to BaO and SO_3 (barite) to confirm statements above. BaO-SO_3-Eu-Sm cluster links to SrO at an elevated distance, implying the secondary

connection to it. This could indicate that REEs (Sm-Eu) enrichment occurred first and followed by the Sr one. The depletion of rare earth elements, prevalence of the light lanthanides over heavy lanthanides, and the positive europium anomaly, are typical of the epithermal ore formation system (**Volkov et al., 2021**).

Fluorite impact

Samples containing higher quantities of fluorite (e.g. Ž-3, Ž-11 and Ž-19) are also showing higher yttrium (Y) concentrations. Although, barite often occurs in sample paragenesis along with fluorite, there is a negative correlation between barite and Y whereas fluorite and Y exhibit positive correlation (**Table 7-1**). Furthermore, the light REEs show a negative correlation and heavy REEs show strong positive correlation with fluorite.

Fluorite is typically associated with several critical elements, among which REEs, Y and Nb, are included. Yttrium is considered to be a pseudo-lanthanide due to its similar size and the same charge as the lanthanides (as referenced in **Magyarosi and Conliffe, 2021**). They emphasized that Y behaves anomalously in F-rich system, and positive Y anomaly is a common feature of hydrothermal fluorites. Ž-3, Ž-11 and Ž-19 sample show slightly positive Y anomaly (**Fig. 6-8**), in contrary to other samples in the deposit. This mild enrichment could be explained by substitution of Ca^{2+} (ionic radius of 1.00 Å) and Y^{3+} (ionic radius of 1.02 Å), and yttrium forming complex with fluorine. As there is a difference in charges between Ca and Y, **Möller et al.** (**1998**) suggested that in order to achieve electrical neutrality, following types of reactions should be considered: (1) $2Ca^{2+} \leftrightarrow REE^{3+} + Na^{+}$; (2) $3Ca^{2+} \leftrightarrow 2\ REE^{3+} + \square$; (3) $Ca^{2+} \leftrightarrow REE^{3+} + F^{-}$. Reaction (3) would be suitable for the previously mentioned substitution, where instead REE^{3+} the Y^{3+} would stand. Except for yttrium, a positive correlation is also observed between HREEs and Na_2O with fluorite. This correlation points us to slightly enrichment of HREEs in fluorites. **Möller et al.** (**1998**) stated that partial dissolution due to tectonic stress and subsequent recrystallization leads to preferred separation of LREE from fluorite. Accordingly, light REEs are predominantly present in a separate phase that has different solubility than fluorite and therefore, due to remobilization, the subsequently precipitated fluorite is considerably depleted in LREE. Also, fractionation of light REEs occurs during precipitation of fluorite due HREE forming more stable fluoro-complexes and staying in the F-rich fluid. At the end, Na (Na_2O in

Table 7-1) positive correlation with HREEs and fluorite can be explained in a way that Na^{+} forms complexes with REE^{3+} while substituting Ca^{2+} according to previously mentioned reaction (1). **Möller et al.** (**1998**) (as referenced in **Magyarosi and Conliffe, 2021**) noted that the positive correlation of Na with the total REE-Y content observed in some phases suggests that the Ca^{2+} atom in the structure of fluorite is replaced by $REE\text{-}Y^{3+}$, with Na^{+} preserving electrical neutral charge in these phases.

An interesting fact was brought up by **Safina et al.** (**2021**) when investigating the chemical composition of fluorite. Yttrium, as important trace element in fluorite, is responsible for colour and luminescence of it. The dependence of the colour of fluorite on the Y content was established at fluorite deposits in Tajikistan where deeply coloured fluorites have high Y concentrations whereas colourless transparent varieties have the lowest Y concentrations (**Safina et al., 2021** and reference therein) with green fluorite richer in Y than purple. In the samples from the Žune deposit, this theory can be implied because samples with highest Y concentrations (Ž-3, Ž-11 and Ž-19 sample) have deep purple colour, while those with low concentrations of Y are usually colourless. In fluorite from the deposits in Tajikistan, the highest concentration of Y was measured (10-400 ppm, average 163 ppm) (as referenced in **Safina et al., 2021**). In fluorite from the Žune deposit concentrations of Y range from 2.90 to 41.60 ppm, average 16.80 ppm. These concentrations of Y measured in analysed Žune samples are similar to those at the North America, Great Britain and Spain deposits where the Y content in fluorite ranges from 5 to 31 ppm (**Safina et al., 2021** and reference therein).

Table 7-5. Correlation table between certain major oxides, trace elements and REEs

	BaO	CaO	MgO	MnO	Na_2O	SrO	Fluor	SO_3	Sm	Eu	Y
BaO	1.00										
CaO	-0.71	1.00									
MgO	-0.67	-0.03	1.00								
MnO	-0.67	-0.03	0.99	1.00							
Na_2O	-0.34	0.90	-0.45	-0.45	1.00						
SrO	0.99	-0.74	-0.64	-0.63	-0.38	1.00					
Fluor	-0.30	0.88	-0.50	-0.50	0.99	-0.34	1.00				
SO_3	1.00	-0.71	-0.68	-0.67	-0.34	0.99	-0.30	1.00			
Sm	0.99	-0.73	-0.66	-0.66	-0.36	0.99	-0.32	0.99	1.00		
Eu	0.99	-0.73	-0.66	-0.66	-0.36	0.99	-0.32	0.99	0.99	1.00	
Y	-0.21	0.83	-0.56	-0.55	0.98	-0.25	0.98	-0.21	-0.24	-0.24	1.00

8. Conclusion

In this master's thesis special attention was put on Žune ore deposit as part of the Ljubija ore deposits. It is hosted by Upper Paleozoic dolostone within a fault zone in contact with Lower Triassic schists and sandstones. Dolostone is considered to belong to the Blagaj formation, an olistostromatic unit of Devonian, Lower to Middle Carboniferous age. Dolostone is dark to light grey in colour and is characterized by massive, homogenous structure. Although dolostone is mostly fresh, limonitization occurs proximal to mineralization. It is composed predominantly of dolomite mineral grains with negligible amount of muscovite. When it comes to geochemical composition, dolostone shows high CaO (30.24–32.38 mass. %), MgO (15.62–17.35 mass. %), LOI (43.61–45.58 mass. %) and low SiO_2 (1.33–3.65 mass. %), Al_2O_3 (0.27–0.74 mass. %) and BaO (0.02–0.83 mass. %) contents. Sum of REEs in dolostone ranges from 5.73 to 18.75 ppm with low Sr (61.70–120.40 ppm), Sm (0.32–2.02 ppm) and Eu (0.08–0.64 ppm). On the contrary, there is an enrichment in Mn (5.00–826.00 ppm), and Ni (7.10–210.90 ppm) in minority, with strong indication of Mn substituting Mg in dolomite crystal lattice.

Contact zone is characterized with presence of primary accessory minerals like tremolite, magnesiochloritoid, pyknite and epidote implying higher forming temperatures that go above 300°C with pressure up to 2 kbars. Data obtained through this study matches to previously

reported high temperatures determined by fluid inclusion studies. X-ray analysis confirmed presence of dolomite, calcite, fluorite with quartz and chloritoid in minority.

Two types of mineralization are present in the deposit, Ba-F vein type as the dominant one, and hydrothermal breccia. Ba-F vein type mineralization is represented by three veinlet subtypes: barite-fluorite-quartz-pyrite, carbonate-quartz/fluorite-limonite and carbonate-limonite veinlets. Hydrothermal breccia is composed mostly out of course-grained barite and fluorite, alongside dolostone fragments, pointing to hydraulic fracturing. Breccia occupies about 20 % of the deposit. Quartz, carbonates and pyrite are accessory minerals in both ore types. Ore samples show low content of Al_2O_3 (0.09–0.38 mass. %) and slightly elevated content of SiO_2 (2.92–5.77 mass. %) compared to barren samples with high BaO (up to 50.74 mass. %), CaO (up to 66.03 mass. %) and low MgO (down to 0.02 mass. %), and LOI (0.30–3.10 mass. %). The sum of REEs ranges from 19.50 to 166.01 ppm in mineralized samples with high Sr (> 1 mass. %), Sm (8.88–118.28 ppm) and Eu (3.29–43.53 ppm) concentrations. Most of the samples show positive Eu and Sm anomaly among which Ž-7, Ž-16 and Ž-19 samples show deviating trend that the rest. These anomalies correspond and correlate positively with amount of barite in the samples and indicate Eu-Sm enrichment in barite. Elevated concentrations of Sr are typical for epigenetic barite hydrothermal deposits in the Dinarides as Ba-Sr substitution occur in barite crystal lattice. Samples containing higher fluorite content are characterized by enrichment in Y (5.50– 41.60 ppm) and HREEs, and depletion on LREEs.

The Mn and Ni substitutions in dolomite are confirmed by hierarchical cluster analysis due to establishment of positive correlation between Mg with Mn and Ni. MgO is further clustered with Al_2O_3, Fe_2O_3 and certain REE (La, Ce, and Pr). Barite indicating cluster is the one where BaO and SiO_2 are forming cluster with SrO, SO_3 and LREEs, Sm and Eu. CaO and Na_2O oxides are clustered together with F, Y and other REEs that refer to fluorite cluster.

Žune Ba-F epithermal deposit, having variable REE concentration and low to moderate negative cerium and ytterbium anomaly correspond to the fluorite deposits associated with carbonate sedimentary rocks according to classification scheme.

9. References

ANDERS, E. & GREVESSE, N., (1989): Abundances of the elements: meteoric and solar. Geochimica et Cosmochimica Acta, 53(1), str. 197-214.

ARNASON, J.G., BIRD, D.K. & LIOU, J.G., (1993): Variables Controlling Epidote Composition in Hydrothermal and Low-Pressure Regional Metamorphic Rocks. Abhandlungen der Geologischen Bundesanstalt, 49, str. 17-25.

AUSTEN, K.F., WRIGHT, K., SLATER, B. & GALE, J.D., (2005): The interaction of dolomite surfaces with metal impurities: a computer simulation study. Physical Chemistry Chemical Physics, 24(7), str. 4150-4156.

BAU, M. & MÖLLER, P., (1992): Rare earth element fractionation in metamorphogenic hydrothermal calcite, magnesite and siderite. Mineralogy and Petrology, 45(3/4), str. 231-246.

BIRD, D.K. & SPIELER, A.R., (2004): Epidote in Geothermal Systems. Reviews in Mineralogy and Geochemistry, 56(1), str. 235-300.

BUCHER, K. & FREY, M., (2002): Petrogenesis of Metamorphic Rocks. Berlin: Springer-Verlag.

CARUSO, L.J., BIRD, D.K., CHO, M. & LIOU, J.G., (1988): Epidote-Bearing Veins in the State 2-14 Drill Hole: Implications for Hydrothermal Fluid Composition. Journal of Geophysical Research, 93(B11), str. 13123-13133.

CHOPIN, C. & SCHREYER, W., (1983): Magnesiocarpholite and magnesiochloritoid: Two index minerals of pelitic blueschists and their preliminary phase relations in the model system MgO-Al_2O_3-SiO_2-H_2O. American Journal of Science, 238A, str. 72-96.

CISSARZ, A., (1951): Die Stellung der Lagerstätten Jugoslaviens im geologischen Raum. Geološki vjesnik IX, str. 23-60.

COOK, S.J. & BOWMAN, J.R., (2000): Mineralogical Evidence for Fluid–Rock Interaction Accompanying Prograde Contact Metamorphism of Siliceous Dolomites: Alta Stock Aureole, Utah, USA. Journal of Petrology, 41(6), str. 739-757.

DEER, W.A., HOWIE, R.A. & ZUSSMAN, J., (1997): Rock-forming minerals. London: The Geological Society of London.

EGGERT, R.G. & KERRICK, D.M., (1981): Metamorphic equilibria in the siliceous dolomite system: 6 kbar experimental data and geologic implications. Geochimica et Cosmochimica Acta, 45(7), str. 1039-1049.

GHENT, E.D, STOUT, M.Z. & FERRI, F., (1989): Chloritoid-paragonite-phyrophyllite and stilpnomelane bearing rocks near Blackwater Mountain, western Rocky Mountains, British Columbia. The Canadian Mineralogist, 27(1), str. 59-66.

GRUBIĆ, A., CVIJIĆ, R., MILOŠEVIĆ, A. & ČELEBIĆ, M., (2015): Importance of olistostrome member for metallogeny of Ljubija iron ore deposits. Archives for Technical Sciences, 13(1), str. 1-8.

HAJALILOU, B., VUSUQ, B. & MOAYED, M., (2014): REE Geochemistry of Precambrian Shale-Hosted Barite-Galena Mineralization, a Case Study from NW Iran. Iranian Journal of Crystallography and Mineralogy, 22(2), str. 39-48.

JANKOVIĆ, S., (1974): Metallogenic provinces of Yugoslavia in time and space. U: Metallogeny and concepts of the geotectonic evolution of Yugoslavia. Belgrade: Faculty of Mining and Geology, str. 37-63.

JANKOVIĆ, S., (1977): Major Alpine deposits and metallogenic units in the NE Mediterranean and concepts of plate tectonics. U: Metallogeny and plate tectonics in the NE Mediterranean, UNESCO/IGCP. Belgrade: Faculty of Mining and Geology, str. 105-172.

JANKOVIĆ, S., (1982): Yugoslavia. U: Mineral deposits of Europe, Vol. 2. Southeast Europe. Mineralogical Society and Institute of Mining and Metallogeny, str. 143-198.

JANKOVIĆ, S., (1987): Genetic types of the Alpine ore deposits and their tectonic settings in the Northeastern Mediterranean and Southwest Asia. U: Geotectonic Evolution and Metallogeny of the Mediterranean Area and Western Asia. Wien: Springer-Verlag, str. 23-26.

JANOUŠEK, V., FARROW, C.M. & ERBAN, V., (2006): Interpretation of whole-rock geochemical data in igneous geochemistry: introducing Geochemical Data Toolkit (GCDkit). Journal of Petrology, 47(6), str. 1255-1259.

JEREMIĆ, M., (1958): Baritno-fluoritno ležište Žune kod Ljubije. Ljubljana: Rudarsko-metalurški zbornik, 4.

JURIĆ, M., (1971): Geologija područja Sanskog paleozoika u sjeverozapadnoj Bosni. Sarajevo: Posebno izdanje Geološkog glasnika XI.

JURKOVIĆ, I., GARAŠIĆ, V. & HRVATOVIĆ, H., (2010): Geochemical characteristics of barite occurrences in the Palaeozoic complex of South-eastern Bosnia and their relationship to the barite deposits of the Mid-Bosnian Schist Mountains. Geologia Croatica, 63(2), str. 241-258.

KARAMATA S., KRSTIĆ B., DIMITRIJEVIĆ M.D., DIMITRIJEVIĆ M.N., KNEŽEVIĆ V., STOJANOV, R. & FILIPOVIĆ, I., (1997): Terranes between the Moesian Plate and the Adriatic Sea. Annales Géologiques des Pays Helléniques, 37(1), str. 429-477.

KATZER, F., (1910): Die Eisenerz lagerstätten Bosniens und der Herzegovina. Wien.

KUBAT, I., (1982): Metalogenija i prognoza čvrstih mineralnih sirovina u trijasu Bosne I Hercegovine. Sarajevo: Posebno izdanje Geološkog glasnika 18.

LIVI, K.J.T., FERRY, J.M., VEBLEN, D.R., FREY, M. & CONNOLLY, J.A.D., (2002): Reactions and physical conditions during metamorphism of Liassic aluminous black shales and marls in central Switzerland. European Journal of Mineralogy, 14(4), str. 647-672.

MAGOTRA, R., NAMGA, S., ARORA, N. & SRIVASTAVA, P.K., (2017): New Classification Scheme of Fluorite Deposits. International Journal of Geosciences, 8(4), str. 599-610.

MAGYAROSI, Z. & CONLIFFE, J., (2021): REE-Y patterns and fluid inclusion analysis of fluorites from the AGS fluorite deposit, St. Lawrence, Newfoundland. Newfoundland and Labrador Department of Industry, Energy and Technology Geological Survey, Report 21(1), str. 27-47.

MAJER, V., (1964): Petrografija paleozojskih sedimenata sjeveroistočnog dijela Trgovske gore. Geološki vjesnik, 17, str. 79-92.

MÖLLER, P., BAU, M., DULSKI, P. & LÜDERS, V., (1998): REE and yttrium fractionation in fluorite and their bearing on fluorite formation. U: Proceedings of the Ninth Quadrennial IAGOD Symposium, Beijing. Beijing: International Association on the Genesis of Ore Deposits, IAGOD, 1998, str. 575-592.

MORGAN, J.W. & WANDLESS, G.A., (1980): Rare earth element distribution in some hydrothermal minerals: evidence for crystallographic control. Geochimica et Cosmochimica Acta, 44(7), str. 973-980.

NÖTH, (1952): Die Eisenerzlagerstätten Jugoslawiens. Belgrade.

PALINKAŠ, A.L., (1985): Lead isotopes patterns in galenas from some selected ore deposits in Croatia and NW Bosnia. Geološki vjesnik, 38, str. 175-189.

PALINKAŠ, A.L., (1988): Geokemijske karakteristike paleozojskih metalogenetskih područja: Samoborska gora, Gorski Kotar, Lika, Kordun i Banija. Dissertation. Zagreb: University of Zagreb.

PALINKAŠ, A.L., (1990): Siderie-barite-polysulfide deposits and early continental rifting in Dinarides. Geološki vjesnik, 43, str. 181-185.

PALINKAŠ, A.L., BOROJEVIĆ ŠOŠTARIĆ, S., STRMIĆ PALINKAŠ, S., PROCHASKA, W. & CUNA, S., (2010): Permian polysulfide-siderite-barite-haematite deposit Rude in Samoborska Gora Mts., Zagorje-Mid-Transdanubian zone of Internal Dinarides. Geologia Croatica, 63(1), str. 93-115.

PALINKAŠ, A.L., BOROJEVIĆ ŠOŠTARIĆ, S., STRMIĆ PALINKAŠ, S., PROCHASKA, W., PÉCSKAY, Z., NEUBAUER, F. & SPANGENBERG, J.E., (2016): The Ljubija geothermal field: A herald of the Pangea break-up (NW Bosnia and Herzegovina). Geologia Croatica, 69(1), str. 3-30.

PAMIĆ, J., (1993): Eoalpine to Neoalpine magmatic and metamorphic processes in the northwestern Vardar Zone, the easternmost Periadriatic Zone and the southwestern Pannonian Basin. Tectonophysics, 226(1-4), str. 503-518.

PAMIĆ, J. AMIĆ, J., GUŠIĆ, I. & JELASKA, V., (1998): Geodynamic evolution of the central Dinarides. Tectonophysics, 297(1-4), str. 251-268.

PAMIĆ, J. & JURKOVIĆ, I., (2002): Paleozoic tectonostratigraphic units of the northwest and central Dinarides and the adjoining South Tisia. International Journal of Earth Sciences, 91, str. 538−554.

SAFINA, N.P., SOROKA, E.I., ANKUSHEVA, N.N., KISELEVA, D.V., BLINOV, I.A. & SADYKOV, S.A., (2021): Fluorite in Ores of the Saf'yanovka Massive Sulfide Deposit, Central Urals: Assemblages, Composition, and Genesis. Geology of Ore Deposits, 63(2), str. 118-137.

SCHMID, S.M., BERZA, T., DIACONESCU, V., FROITZHEIM, N. & FÜGENSCHUH, B., (1998): Orogen-parallel extension in the Southern Carpathians. Tectonophysics, 297(1), str. 209-228.

SLAUGHTER, J., KERRICK, D.M. & WALL, V.J., (1975): Experimental and thermodynamic study of equilibria in the system $CaO–MgO–SiO_2–H_2O–CO_2$. American Journal of Science, 275(2), str. 143-162.

SLOVENEC, D., (2002): Sistematska mineralogija: interna skripta. Zagreb: Rudarsko-geološko-naftni fakultet.

SRIVASTAVA, P.K. & SUKCHAIN, (2005): Petrographic Characteristics and Alteration Geochemistry Granite-hosted Tungsten Mineralization at Degana, NW India. Resource Geology, 55(4), str. 373-384.

STATSOFT, INC., (2012): Electronic Statistics Textbook. Tulsa, OK: StatSoft. Available form: <http://www.statsoft.com/textbook/>.

TAYLOR, S.R. & MCLENNAN, S.M., (1995): The geochemical evolution of the continental crust. Reviews of Geophysics, 33(2), str. 241-265.

THOMAS, R., (1994): Fluid evolution in relation to the emplacement of the Variscan granites in the Erzgebirge region: A review of the melt and fluid inclusion evidence. U: Metallogeny of Collisional Orogens. Prague: Czech Geological Survey, 1994, str. 70-81.

TOMLJENOVIĆ, B., (2002): Strukturne značajke Medvednice i Samoborskog gorja. Dissertation. Zagreb: University of Zagreb.

VOLKOV, A.V, SAVVA, N.E., ISHKOV, B.I., SIDOROV, A.A., KOLOVA, E.E. & MURASHOV, K.Y., (2021): Burgali Epithermal Au-Ag Deposit in the Paleozoic Kedon Volcanic Belt (Northeastern Russia). Geology of the Ore Deposits, 63(1), str. 34-53.

WILLINGSHOFER, E., (2000): Extension in collisional orogenic belts: the Late Cretaceous evolution of the Alps and Carpathians. PhD Thesis. Amsterdam: Vrije University.

WRIGHT, J.H. & KWAK, T.A.P., (1989): Tin-bearing greisens of Mount Bischoff, northwestern Tasmania, Australia. Economic Geology, 84(3), str. 551-574.

ZOU, H., FANG, Y., ZHANG, S-T & ZHANG, Q., (2016): The source of Fengjia and Langxi barite–fluorite deposits in southeastern Sichuan, China: evidence from rare earth elements and S, Sr, and Sm–Nd isotopic data. Geological Journal, 52(3), str. 470-488.

Internet sources:

Geographical position of the study area. URL: https://earth.google.com/web/ (18.10.2021.)